Performance Analysis of a MIMO Optical Wireless link with Space Time Block Code (STBC)

By

Md. Zahirul Islam

Under the supervision of
Professor Dr. Satya Prasad Majumder
BUET

A project Submitted in partial fulfillment of the requirement for the degree of

MASTER OF ENGINEERING
IN
ELECTRICAL AND ELECTRONIC ENGINEERING

DEPARTMENT OF ELECTRICAL AND ELECTRONIC ENGINEERING
BRAC UNIVERSITY

The project titled, "**PERFORMANCE ANALYSIS OF A MIMO OPTICAL WIRELESS LINK WITH SPACE TIME BLOCK CODE (STBC)"** submitted by Md. Zahirul Islam Roll. No. 14171003 session 2010-2011 has been accepted as satisfactory in partial fulfillment of the requirement for the degree of Master of Engineering in Electrical and Electronic Engineering on ……..

Board of Examiners

1. _____ Chairman

Dr. Sayeed Salam
Professor and Chairman
Department of Electrical and Electronic Engineering
BRAC University

2. _____ Member

Dr. Amitabha Chakrabarty
Assistant Professor
Department of Computer Science and Engineering
BRAC University

3. _____ Member

Dr. Mohammed Belal Hossain Bhuian
Assistant Professor
Department of Electrical and Electronic Engineering
BRAC University

4. _____ Member

Mr. Tarem Ahmed
Senior Lecturer
Department of Electrical and Electronic Engineering
BRAC University

Declaration

This is to certify that project is the result of my study and it has not been submitted elsewhere for any other degree or diploma.

Signature of the candidate

……
(Md. Zahirul Islam)
ID. 14171003

Dedicated to my father

Acknowledgements

All praise to Almighty Allah due to whose benevolence I was able to complete this work. Firstly, I would like to express my deepest gratitude to my supervisor, Dr. Satya Prasad Majumder, Professor, Department of Electrical and Electronic Engineering, Bangladesh University of Engineering and Technology (BUET), Dhaka for his continuous guidance, advice and encouragements. I have been the greatest honor to work with him.

I would also like to thank Prof. Dr. Md. Sayeed Salam, Professor and Chairperson, BRAC University for his support and for permitting me to use all the necessary resources of the department.

I am indebted to my family members, especially to my father for their endless patience, support and encouragement.

Table of Contents

Chapter 3

Chapter 4

Chapter 5

Appendix

List of Abbreviations

SNR	Signal to noise ratio
SI	Scintillation
FSO	Free-Space Optical
BER	Bit error rate
SEP	Symbol error probability
BPSK	Binary phase shift keying
SISO	Single input single output
SIMO	Single input multiple output
MISO	Multiple input single output
MIMO	Multiple –input multiple-output
PPM	Pulse position modulation
FOV	Field of view
IEC	International Electro technical Commission
ANSI	American National Standards Institute
AEL	Allowable Exposure Limit
OOK	On Off keying
IM/DD	Intensity modulation/direct detection
PDF	Probability density function
MRC	Maximal ratio combining
EGC	Equal Gain Combining
OC	Optimal Combining
LOS	Line of Sight
LED	Light-Emitting Diode
APD	Avalanche Photodiode
AWGN	Additive White Gaussian Noise

List of Figures

List of Tables

Abstract

Performance analysis has been carried out for a space time block coded multiple input multiple output (MIMO) optical wireless link considering atmospheric turbulence. The diversity reception in the receiving has been carried out by multiple receiving antennas with maximal ratio combining (MRC) technique. The expression of the receiver output has been derived for several sets of space time block codes considering Rayleigh fading model. The Probability density function (PDF) of the output of the MRC combiner has been developed and is used to find the unconditional average bit error rate (BER). The Performance results are evaluated numerically in terms of BER for several code and system parameters. The improvements in performance of an optical free-space link due to space diversity are determined at given BER. The optimum system design parameters are also determined at a given BER.

Chapter 1

Introduction

CHAPTER 1

INTRODUCTION

1.1 General Perspective:

In recent Years, there has been a migration of computing power from the desktop to portable, mobile formats. Devices such as digital still and video cameras, portable digital assistants and laptop computers offer users the ability to process and capture vast quantities of data. Although convenient, the interchange of data between such devices remains a challenge due to their small size, portability and low cost. High performance links are necessary to allow data exchange from these portable device to established computing infrastructure such as backbone networks data storage device and user interface peripherals [01]. For this purpose, some parts of communication links need to be constructed wireless. During the last decade, therefore, the wireless communication technology has grown rapidly [02]–[04]. The Technology base for implementing this concept does not yet exist, however. Radio technology although well suited for moderate –speed applications such as voice, may not be sufficient to support many high-speed applications.

Table 1.1. Comparison of wireless optical and communication channel

Serial No	Property	Wireless Optical	Radio
1	RF Circuit design	No	Yes
2	Bandwidth regulated	No	Yes
3	Data rate	100's Mbps	10's Mbps
4	Security	High	Low

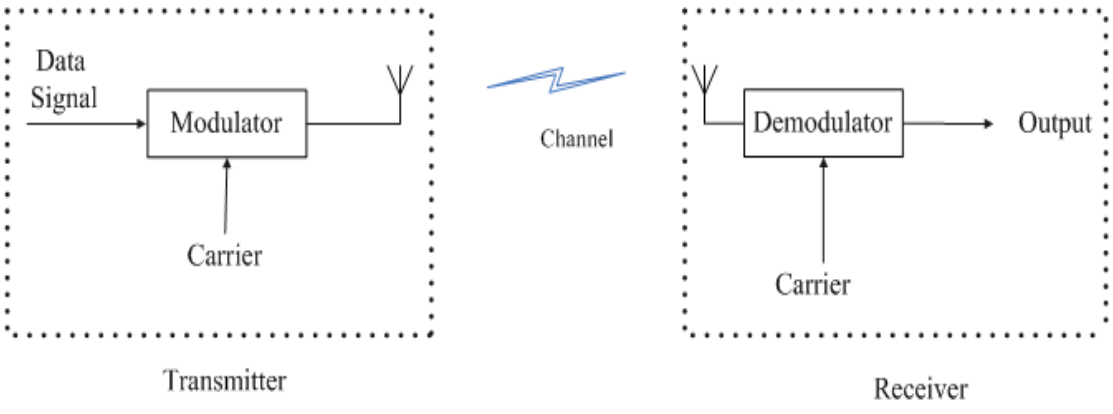

Fig.1.1. Block diagram of a wireless communication system.

1.2 Brief History of optical wireless communication:

In early claude chappe invented the optical telegraph which was able to send message over distances by changing the orientation of signaling arms on a large tower. A code book of orientation of the signaling arms was developed to encode letters of the alphabet, numerals, common works and control signals. Message could be sent over distances of hundreds of kilometers in a matter of minutes [05]. One of the earliest wireless optical communication devices using electronic detectors was the photo phone invented by A.G. Bell and C.S trainer an patented on December 14, 1880. The System is design to transmit a operator s voice over a distance by modulating reflected light from the sun on a foil diaphragm. The receiver consisted of a selenium crystal which converted the optical signal into an electrical current. With this setup, they were able to transmit an audible signal a distance of 213 [06]. Optical transmission came to be available for the communication system after the laser as a light source was invented. As a coherent light source being not in a nature, ruby laser was invented by Dr. T. Mainman in 1960, H- Ne laser oscillated in Bel Labs next year , and GaAs semiconductor laser oscillated in1962. The continuous oscillation of GaAlAs laser was realized in Japan, the United States and the Soviet Union in 1970 and the small semiconductor laser which could be high- speed modulated advanced optical transmission technology greatly. Around from 1965, the beam guide system which arranged the lens in a pipe, and the space propagation system which emits light to free space were beginning to be studied so as to use laser for free space optical communication . In 1979, indoor Bapst [07]. In their system, diffuse optical radiation in the near-infrared region was utilized as signal carrier to interconnect a cluster of terminal located in the same room to a common cluster controller. However the reduction in loss of the fiber and invention of continuous semiconductor laser has moved the mainstream of the research to optical transmission system was accelerated from 1970 to 1980.

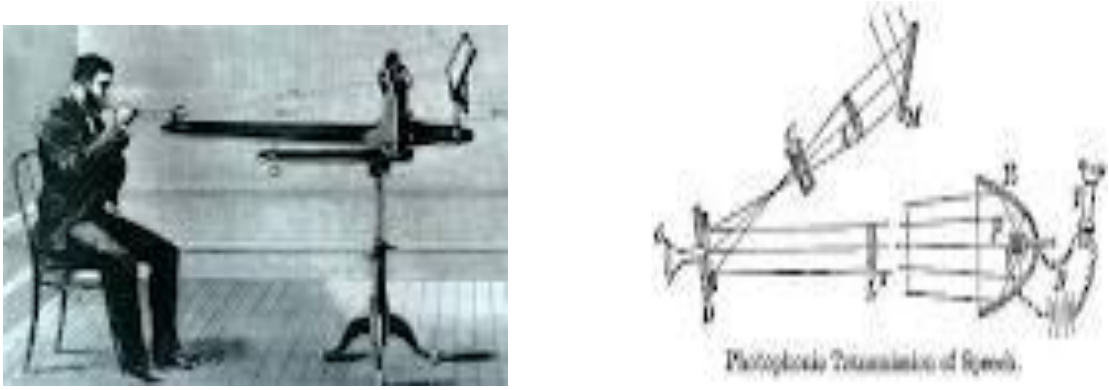

The Photophone, 1880

Fig. 1.2. Alexander Graham Bell’s Photophone, 1880.

1.3 Review of Previous Works

Free-space optical (FSO) Communication has received considerable attention recently as an effective means of transferring data at high rates over shorts distances. Its advantages are that it is rapidly deployable, lightweight and of high capacity without licensing fees and tariffs [08]. However, FSO systems suffer from the degrading effects of atmospheric turbulence, pointing errors and other's errors. Various statistical models have been proposed to describe atmospheric turbulence for varying strength. Although the log-normal model is often used to model weak turbulence , the gamma-gamma model has recently become popular, because of its excellent fit with measurement data for a wide range of turbulence conditions (Weak to strong) [09],[10]. In [11], Uysal, Li and Yu have used this channel model to evaluate the performance of coded FSO links in terms of the pair-wise probability and BER. Popoola et al. in [12] have used this model to study the error performance of a FSO system using subcarrier intensity modulation based on a binary phase shift keying (BPSK) scheme. In [13] Nazmul and Prasad have used this model to evaluate the bit error rate performance degradation of a wireless optical link in the presence of atmospheric scintillation based on OOK, BPSK, QPSK and Q-ary PPM Schemes. The effects of misalignment on FSO systems have been investigate by Arnon and kedar in [14-16]. In these works , the detector aperture size has been considered negligible in comparison to the beam width at the receiver. The combined effect of pointing error and atmospheric turbulence have been investigated for the first time in [14] where Arnon obtain a BER model taking into account both building sway and turbulence–induced log amplitude fluctuations. In [17] Farid and Hranilovic have provided a FSO channel model which models the fading due to atmospheric turbulence and misalignment considering beam width, pointing error variance and detector size. In their model, the channel fading coefficient due pointing error, h_p is distributed as

$$f_h(h) = \frac{\gamma^2}{A_o \gamma^2} h^{\gamma^2 - 1} \quad 0 \le h_p \le A_o$$

Where $\gamma = w_{zeq} / 2\sigma_s$ is the ratio between the equivalent beam radius at the receiver and the pointing error displacement standard deviation at the receiver and A_o is the fraction of the power collected without any pointing error. Particularly, they have considered log-normal distributed and gamma-gamma distributed turbulence and have examined the system performance in terms of capacity and outage probability. His model was used by sandalidis et al in [18] to evaluate the BER performance of a FSO link over a K- distributed strong turbulence channel together with pointing errors.

Recently, It has been shown that the effect of turbulence induced fading in FSO systems is greatly reduced by the use of multiple lasers at the transmitter and multiple photodetectors at the receiver [19-26]. In [19], simulated BER performance results are demonstrated for a dual receiver FSO link in log-normal turbulence.

In [20], [21], Shin and Chan considered spatial diversity at both the transmitter and receiver are found that using diversity can significant reduce the outage probability and provide significant power gain over the non-diversity system. In [22],[23] Wilson

et al. have studied multiple input multiple output (MIMO) FSO transmission assuming pulse position modulation (PPM) [23] and Q-ary PPM [23] both in lognormal and Rayleigh fading regimes.

In[24], Navidpour et al. have investigated the BER performance of FSO links with spatial diversity over log-normal atmospheric turbulence fading channels, assuming both independent and correlated channels among transmitter/receiver apertures. They found the efficient separation between apertures and strict co-alignment is crucial to achieve the promised diversity. In [25], Tsiftsis et al. investigate the performance of multiple input multiple output (MIMO) FSO links over independent and not necessarily identical K-turbulence channels by obtaining closed-form expressions of the BER in terms of MEijer G-function. Bayaki et al. evaluate the performance of MIMO FSO links over gamma-gamma fading channels in [26] by expressing the PEP as a generalized infinite power series with respect to the signal to noise ration (SNR). The results of [25] and [26] demonstrate that the use of multiple apertures at the transmitter and /or receiver enhance the quality of FSO systems similar to RF ones.

A. G. Zambrana [27], have analyzed the error rate performance for space-time block coding (STBC) in free space optical (FSO) communication systems with direct detection operating over strong atmospheric turbulence channel. X. Wu and P. Liu [28], have discussed the both turbulence-induced intensity fluctuations and the angle of arrival effects in full free- space optical communication systems which are used in a few kilometers communication.

1.4 Objectives:

1. To evaluate the Performance result considering diversity reception in the receiver with maximal ratio combining (MRC) Technique.
2. To derive the expression of the receiver output for several sets of space time block codes considering Rayleigh fading model.
3. To find the expression of the conditional bit error rate (BER) for a given Atmospheric Turbulence for MIMO, MISO, SIMO and SISO configuration.
4. To find the unconditional average bit error rate (BER).
5. To evaluate the performance the result numerically in terms of BER for several code and system parameters.
6. To determine the optimum system design parameters at a given BER.

1.5 Organization of the Thesis:

Chapter 1 gives the introduction to FSO communication and briefly describes its limitation. Review of previous works done on FSO in relation to atmospheric turbulence, pointing error and spatial diversity are also discussed in this chapter.

In chapter 2, a brief overview of different component and different terminologies used in FSO communication is discussed. The description of spatial diversity in FSO or MIMO FSO is also discussed in this Chapter.

In chapter 3 theoretical analysis for the system without and with diversity and space time block code in a free space optical link is presented in the presence of atmospheric turbulence.

In chapter 4 the numerical computations are presented obtained by performance results.

Finally, some conclusion and suggestions for future work are provided in Chapter 5.

Chapter 2

Optical wireless communication systems

CHAPTER 2

OPTICAL WIRELESS COMMUNICATION SYSTEMS

2.1 Introduction

This chapter introduces some basic concepts used in the following chapters which are required for the understanding of this work. We begin with the importance of free space optical communication in section 2.2.Understanding the performance of FSO link in section 2.3. A review of the brief description of major components of a optical wireless link comes next in section 2.4. In section 2.5 describes the characteristics of difference channel topologies and their relative advantage and disadvantage.

2.2 Importance of free-space optical communication

Communication systems transmit information from a transmitter to a receiver through the construction of a time- varying physical quantity or a signal. A familiar example of such a system is a wired electronic communication in which information is conveyed from the transmitter by sending an electrical current or voltage signal through a conductor to a receiver circuit. Another example is wireless radio frequency (RF) Communications in which a transmitter varies the amplitude, phase and frequency of an electromagnetic carrier which is detected by a receive antenna and electronics. In each of this communication system's the transmitted signal is corrupted by deterministic and random distortions due to the environment. For example wired electrical communication systems are often corrupted by random thermal as well as shot noise and often frequency selective. These distortions due to external factors are together referred to as the response of a communications channel between the transmitter and receiver. For the purpose of system design, the communications channel between is often represented by a mathematical model which is realistic to the physical channel. The goal of communication system design is to develop signaling techniques which are able to transmit data reliable and at high Rates over these distorting channels. As a medium for wireless communication Light wave radiation offers several significant advantages over radio. Light wave emitters and detectors capable of high speed operation are available at low cost. The light wave spectral region offers a virtually unlimited bandwidth that is unregulated worldwide. Infrared and visible light are close together in wavelength, and they exhibit qualitatively similar behavior. Both are absorbed by dark objects, diffusely reflected by light colored objects, and directionally reflected from shiny surfaces. Both types of light penetrate through glass, but not through walls or opaque barriers, so that optical wireless communications are confirmed to the room in which they originate. This signal confinement makes it easy to secure transmissions against casual eavesdropping, and it prevents interference between links operating in. different rooms. Thus, Optical wireless networks can potentially achieve a very high aggregate, capacity, and their design may be simplified, since transmissions in different rooms need not be coordinated. When an optical wireless link employs intensity modulation with direct detection (IM/DD), the short carrier wavelength and large-area square-law detector lead to efficient spatial diversity that prevents multi-path fading. By contrast,

radio links are typically subject to large fluctuation in received signal magnitude and phase. Freedom from multi-path fading greatly simplifies the design of the optical wireless link. The light wave is not drawbacks however. Because light wave cannot penetrate walls, communication from one room to another requires the installation of optical wireless access points that are interconnected via a wired backbone. In many applications, there exists intense ambient light noise, arising from sun-light incandescent lighting and fluorescent lighting, which induce noise in an optical wireless receiver. In virtually al short-range, indoor applications IM/DD is the only practical transmission technique. The signal-to-noise (SNR) of a direct detection receiver is proportional to the square of the received optical power, implying that IM/DD links can tolerate only a comparatively limited path loss. Often optical wireless link must employ relatively high transmit power levels and operate over a relatively limited range. While the transmit power level can usually be increased without fear of interfering with other users, transmitter power may be limited by concern of power consumption and eye safety, particularly in portable transmitters [28].

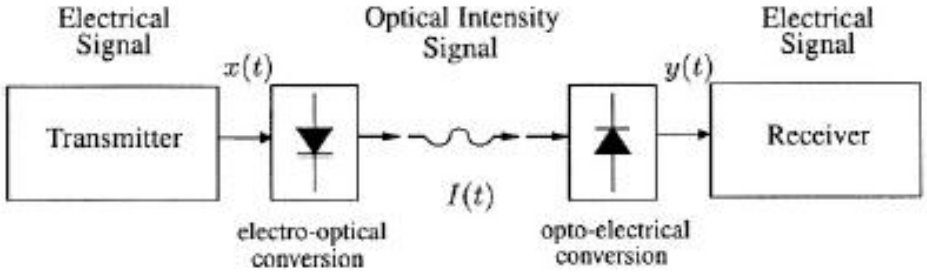

Fig. 2.1. Block diagram of optical intensity, direct detection communication channel

2.3 Understanding the performance of FSO

Several System Parameters, Internal and External need to be taken into account when considering the performance of free-space optics. Internal parameters are related to the design of a FSO system and include optical power, wavelength, transmission bandwidth, divergence angle and optical loss on the transmit side [29]. On the receiver side, it includes receiver sensitivity, BER, receiver lens diameter and receiver field of view (FOV). External parameters are related to the environment in which the system must operate and includes atmospheric attention, turbulence, deployment distance and pointing error.

2.4 Brief Description of Major Components of an Optical Wireless Link

An optical wireless links consists of a transmitter, wireless communication channels and a receiver as shown in figure. 2.2 and 2.3.

2.4.1 Optical Sources

In most optical communication systems, semiconductor light sources are used to convert electrical signals into light. Optical sources for wireless transmission must be compatible to overcome the atmospheric effects and they should be such that one can easily modulate the light directly at high data rates. Generally either Lasers or LEDs are used in optical communication systems [28].

2.4.1.1 LED

Light emitting diodes (LEDs) used in optical communication system are the same as visual display LEDs expect that they operate in the infra-red region and with many times higher intensity of emission. When the p-n junction is forward biased, photon emission takes place due to recombination of electron-hole pair. The wavelength of emission will depend on the energy gap [28].

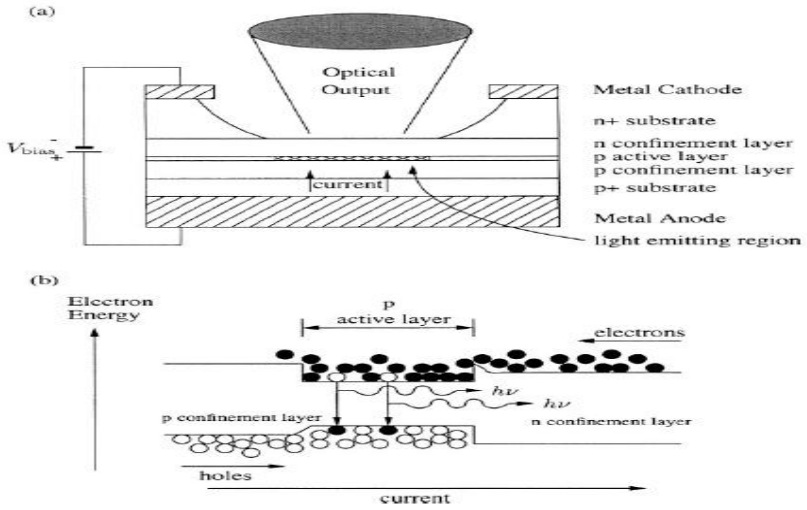

Fig. 2.2. A double heterostructure LED (a) construction and (b) band diagram under forward bias

2.4.1.2 LASER

Laser stands for "Light amplification by stimulating emission of radiation". Compared to LED, a laser has wider bandwidth, higher power output, higher modulation efficiency, narrower spectral line-width and narrower emission pattern. Laser sources are much brighter than LEDs [28].

2.4.2 Optical Detectors

An optical detector is a photon to electron converter. Avalanche photo-diode (APD) and positive intrinsic negative (PIN) diode is the most commonly used detectors. The most important thing of the optical communication system is that the spectral response of both the source and the detector must be same; otherwise efficiency will suffer [28].

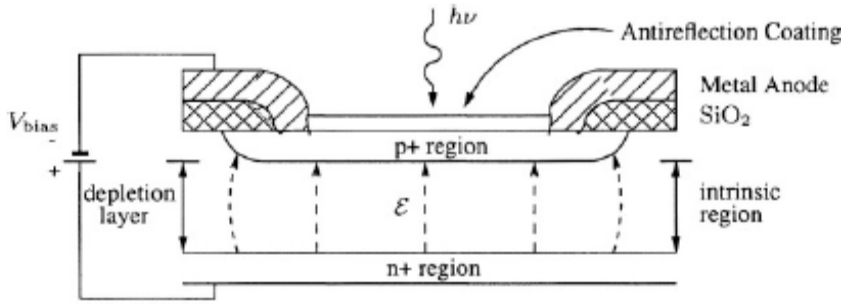

Fig. 2.3. Structure a simple silicon p-i-n photodiode

2.4.2.1 PIN Photo detector

PIN photo detector is the simplest optical detector. It is composed of an n^+ substrate, a lightly doped intrinsic region and a thin p zone. Operated with a reverse bias, mobile carriers leave the p-n junction producing a zone of moderate electric field on both sides of the junction into the intrinsic region. As it only lightly doped, this field extends deeply. Incident light power is mainly absorbed in the intrinsic region, causing electron hole pairs to be generated. These carriers are separated by the influence of the electric field in the intrinsic and represent a reverse diode current can be amplified [28].

2.4.2.2 APD Photo detector

It is the second popular type of photo detector and has the advantage of internally multiplying the primary detected photo current by avalanche process, thus increasing the signal detection sensitively. But some noise is also generated here. The frequency response of both PIN and APD are similar, making them both suitable up to 1 GHz. The main advantage of APD over PIN diode is greater gain bandwidth product due to the inbuilt gain. Silica is the material used at short wavelength (< 1 nm), GE, InGaAsP and AlGaAsP becoming popular at the longer wavelength around 1.3 m [28].

2.5 Channel Topologies

The characteristics of the wireless optical channel can vary significantly depending on the topology of the link considered. This section presents three popular wireless optical channel topologies and discusses the channel characteristics of each [29].

2.5.1 Point -to-Point Links

Point-to-Point wireless optical links operate when there is a direct unobstructed path between a transmitter and a receiver. Figure 2.4 present a diagram of a typical point-to-point wireless optical link. A link is established when the transmitter is oriented toward the receiver. In narrow field –of-view applications this oriented configuration allows the receiver to reject ambient light and achieve high data rates and low path loss. The main disadvantage of this link topology is that it requires pointing and sensitive to blocking and shadowing. The frequency response of these links is limited primarily by front-end photodiode capacitance. Since inexpensive large-area photodiodes are typically used with limited reverse bias the depletion capacitance significantly limits the link bandwidth [30].
A typical example of these links is the standard infrared Data Association (IrDa) Fast IR 4 Mbps link. These links offer communication over 1 m of separation and are used primarily for data interchange between portable devices. The achievable bandwidth in this inexpensive system is on the order of 10-12 MHz which is approximately three orders of magnitude smaller than in wired fiber–optic systems. New IrDA point-to-point links operating at 16 Mbps have also been standardized and may begin appearing in a wider range of application. Another

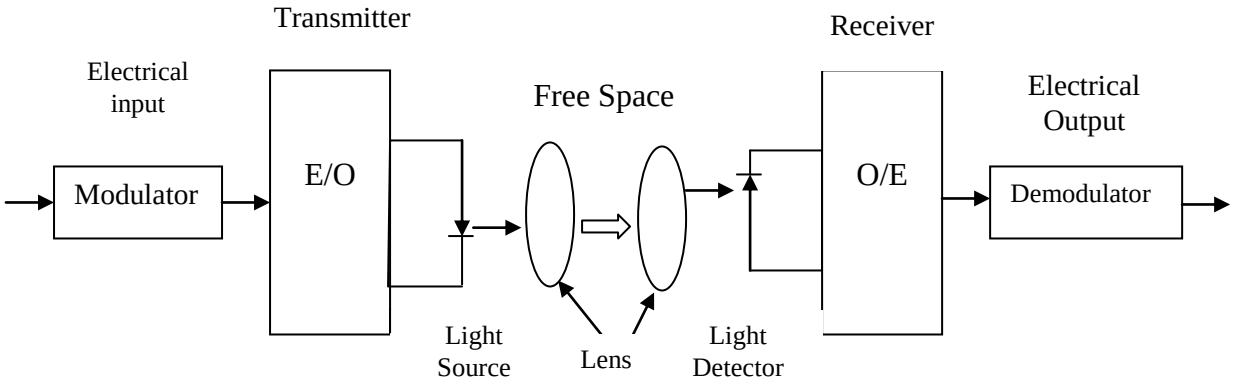

Fig. 2.4. Block diagram of point to point Optical link.

Channel topology which uses a number of parallel point-to-point links is the space division multiplexing architecture. Space division multiplexing is a technique by which a transmitter outputs different data in different spatial directions to allow for the simultaneous use of one wavelength by multiple users. In one such system a ceiling-mounted base station has a number of narrow beams establishing point-to-point links in a variety of direction in a room. A fixed receiver once aligned to within 1 of a transmitter beam establishes a high speed link at up to 50 Mbps. Another means of implementing a space division multiplexing system the transmitter beams are steer

able under the control of a tracking subsystem. Tracking is typically accomplished by a beacon LED or FM transmitter on the mobile terminal. These systems are proposed to provide 155 Mb/s ATM access to mobile terminals in a room. Electronic tracking systems have also been proposed which exploit a diffuse optical channel to aid acquisition. The advantage of this topology is that it is extremely power efficient and supports a large aggregate bandwidth inside of a room at the expense of system complexity. Point-to-point wireless optical links have been implemented in a wide variety of short and long range applications. Short range infrared band links are being designed to allow for the transfer of financial data between a PDA or cell phone and a point-of-sale terminal. Wireless optical links are chosen as the transmission medium due to the low cost of the transceiver and security available by confining optical radiation. The IrDA has specified a standard for this financial application under the title IrDA FM (Financial message). Medium range indoor links have also been eloped to extend the range of Ethernet networks in an office environment. A 10 Mbps point-to-point wireless infrared links to extend Ethernet networks has been deployed over a range of at most 10 m. Higher rate 100 Mbps point-to-point wireless infrared links have also been designed to extended Ethernet networks in indoor.

2.5.2 Diffuse Links

Diffuse Transmitters radiate optical power over a wide solid angle in order to ease the pointing and shadowing problems of point-to-point links. Figure 2.5 presents a block diagram of a diffuse wireless optical system. The transmitter does not need to be aimed at the receiver since the radiant optical power is assumed to reflect from the surface of the room. The afford user terminals wide degree of mobility at the expense of a high path loss. These channels however suffer not only from optoelectronic bandwidth constraints but also from low-pass multipath distortion [31]. Unlike radio frequency wireless channels diffuse channels do not exhibit fading. This is due to the fact that the receiver photodiode integrates the optical intensity field over an area of millions of square wavelengths and hence no chance in the channel response is noted if the photodiode is moved a distance on the order of a wavelength [32]. Thus the large size of the photodiode relative to the wavelength of light provides a degree of spatial diversity which eliminates multipath fading. Multiath distortion gives rise to a channel bandwidth limit of approximately 10-2000 MHz depending on room layout shadowing and link configuration [32-33]. Many channel models based on measurements allow for the accurate simulation of the low-pass frequency response of the channel. The IrDA and the IEEE have similar standards for diffuse infrared links. The IrDA Advanced Infrared (AIr) standard allows communication at rates up to 4 Mbps with repetition coding. The IEEE wireless infrared standard falls under the 802.11 standard and allows diffuse transmission at a maximum of 2 Mbps. Both systems used pulse-position modulation (PPM) which is a coded version of On-Off keying. Experimental indoor wireless optical links have been demonstrated at 50 Mbps using on-off keying over a horizontal range of approximately 3 m. A commercial indoor diffuse wireless optical link aimed at digital audio and set-top box applications claims data rates of up to 5 Mbps in typical indoor environments.
An early diffuse wireless optical system was employed in a portable computer called PARCTAB, developed at the Xeror Palo Alto Research Center (PARC) in 1993. The diffuse link was able to provide data rates of up to 19.2 Kbps and was used to communicate electronic mail and other data to a hand-held computing device.

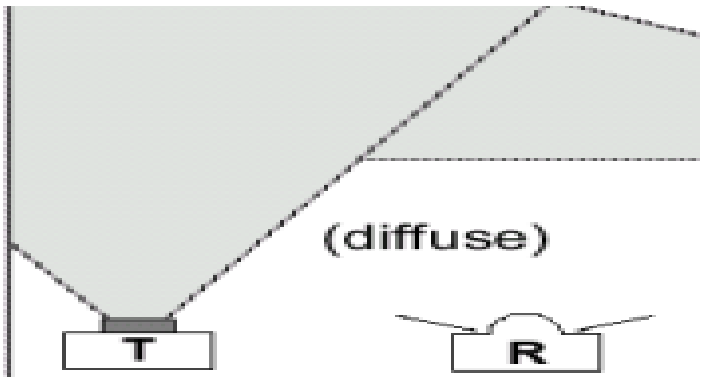

Fig.2.5. A diffuse optical wireless communication system

2.5.3 Quasi-Diffuse Links

The transmitter and illuminates the ceiling with a series of slowly diverging beam sources which illuminates a grid of spots on the ceiling. In experimental settings these multiple beams are created using individual light sources [34] and proposed techniques using holographic beam splitters appear promising [35]. The transmit beams suffer a small path loss nearly independent of the length of the link from the transmitter to the ceiling due to the low beam divergence. The data transmitted on all beams is identical. The receiver consists of multiple concentrator/photodiode pairs each with a non-overlapping narrow FOV of the ceiling. The FOV of each receiver rejects a majority of multipath distortion and provide a link with an improved bandwidth although the link is more sensitive to shadowing relative to diffuse links. Spatially localized interferers such as room illumination can be rejected by using the spatial diversity of the multiple receivers. In a diffuse scheme all the noise power is collected along with the signal power.

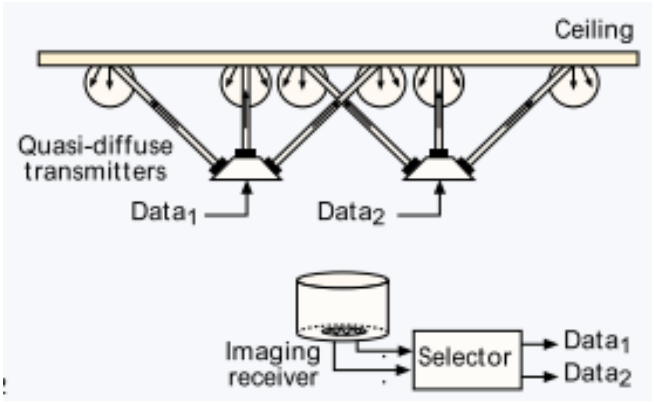

Fig. 2.6. A quasi-diffuse optical wireless communication system.

Table 2.1. Comparison of wireless optical topologies

	Point to point	Diffuse	Quasi-diffuse
Rate	High	Low-Moderate	Moderate
Pointing required	yes	No	Somewhat
Immunity to blocking	Low	High	Moderate
Mobility	Low	High	Moderate
Complexity of optics	Low	Low Moderate	High
Ambient light Rejection	High	Low	High
Multipath Distortion	None	High	Low
Path Loss	Low	High	Moderate

2.4.1 Comparison of Different Technologies

Table 2.1 presents a comparison of some of the characteristics of the three channel topologies discussed. The point to point topology is a low complexity means to achieve high data rate links at the expense of mobility and pointing requirements. Diffuse links suffer from high path loss but offer a great degree of mobility and robustness of blocking. Quasi-diffuse links permit higher data rates by requiring users to aim their receivers at the ceiling but suffer from a higher implementation cost due to the multi-beam transmitter. Thus each channel topology is suited to a different application depending on required data rates and channel conditions. It may also be advantages to combine the operation of the various topologies to form a more robust link. Recent work has demonstrated experimental configuration which use a diffuse wireless optical channel to aid in requiring tracking and to serve as a backup link to improve user mobility [36].

2.6 Eye and Skin safety

Safety considerations must be taken into account when designing a wireless optical link. Since the energy is propagated in a free-space channel, the impact of this radiation on human safety must be consideration. There are a number of international standards bodies which provide guidelines on LED (IEC60825-1), American National Standard Institute (ANSI) (ANSI Z136.1), and European committee for Electrotechnical Standardization (CENELEC) among others. In this section, we will consider the IEC standard which has been widely adopted. This standard classifies the main exposure limits of optical sources. Table 2.2 includes a list of the primary classes under which an optical radiator can fall. Class 1 operation is most desirable for a wireless optical system since emissions from products are safe under circumstances.

Under these conditions, no warning labels need to be applied and device can be used without special safety precautions. This is important since these optical links are destined to be inexpensive, portable and convenient for user. An extension to class 1, termed Class 1M, refers to source which are safe under normal operation but which may be hazardous if viewed with optical instruments [29]. Longer distance free-space links often operate in class 3B mode and are used for high data rate transmission over moderate distances (40 m). The safety of these systems is maintained by locating optical beams on rooftops or on towers to prevent inadvertent interruption [37]. On some longer range links, even through the laser emitter is Class 3B; the system can still be considered Class 1M if appropriate optics are employed to spread the beam over a wide enough angle.

The choice of which optical wavelength to use for the wireless optical link also impacts the AEL. Table 2.3 presents the limits for the averages transmitted optical power for the IEC classes listed in Table 2.2 at four different wavelengths. The allowable average optical power is calculated assuming that the source is a point emitter, in which the radiation is emitted from a small aperture and diverges slowly as is the case in laser diodes. Wavelengths in the 650 nm range are visible red light emitters. There is a natural aversion response to high intensity sources in the visible band which is not present in the longer wavelength infrared band.

Table 2.2: Interpretation of IEC safety classification for optical sources

Safety Class	Interpretation
Class 1	Safe under reasonable foreseeable conditions of operation.
Class 2	Eye protection afforded by aversion responses including blink reflex.
Class 3A	Safe for viewing with unaided eye. Direct intra-beam viewing with optical aids may be hazardous.
Class 3B	Direct intra-beam viewing is always hazardous. Viewing diffuse reflections in normally safe.

The visible band has been used rarely in wireless optical communication applications due to the high background ambient light noise present in the channel. However, these have been some development of visible band wireless optical beams on rooftops or on towers to prevent inadvertent interruption. On some longer range links, even though the laser emitter is class 3B, the system can be beam over a wide enough angle.

The critical parameter which determines whether a source falls into a given class depends on the application. The allowable exposure limit (AEL) depends on the wavelength of the optical source, the geometry of the emitter and the intensity of the source. In general, constraints are placed on both the peak and average optical power emitted by a source. For most practical high frequency modulated sources, the average transmitted power of modulation scheme is more restrictive than the peak power limitation and sets the (AEL) for a given geometry and wavelength [04]. At modulation frequencies greater than about 24 KHz, the AEL can be calculated based on average output power of the source [31].

Eye safety considerations limit the average optical power which can be transmitted. This is another fundamental limit on the performance of free-space optical links.

Table 2.3. Point source safety classification based on allowable average optical power output for a variety of optical wavelengths

Safety	650 nm	880 nm	1310 nm	1550 nm
Class	Visible	Infrared	Infrared	Infrared
Class 1	<0.2 mW	<0.5 mW	<8.8 mW	<10 mW
Class 2	<0.2-1 mW	N/A	N/A	N/A
Class 3A	1-5 mW	0.5-2.5 mW	8.8-45 mW	10-50 mW
Class 3B	5-500 mW	2.5-500 mW	45-500 mW	50-500 mW

2.7 Description the Limitation of Optical Signal With respect to MIMO Technology

2.7.1 MIMO Technology

MIMO (multiple input, multiple output) is an antenna technology for wireless communications in which multiple antennas are used at both the source (transmitter) and the destination (receiver). The antennas at each end of the communications circuit are combined to minimize errors and optimize data speed. MIMO is one of several forms of smart antenna technology, the others being MISO (multiple input, single output) and SIMO (single input, multiple output).

In conventional wireless communications, a single antenna is used at the source, and another single antenna is used at the destination. In some cases, this gives rise to problems with multipath effects. When an electromagnetic field (EM field) is met with obstructions such as hills, canyons, buildings, and utility wires, the wavefronts are scattered, and thus they take many paths to reach the destination. The late arrival of scattered portions of the signal causes problems such as fading, cut-out (cliff effect), and intermittent reception (picket fencing). In digital communications systems such as wireless Internet, it can cause a reduction in data speed and an increase in the number of errors. The use of two or more antennas, along with the transmission of multiple signals (one for each antenna) at the source and the destination, eliminates the trouble caused by multipath wave propagation, and can even take advantage of this effect.

MIMO technology has aroused interest because of its possible applications in digital television (DTV), wireless local area networks (WLANs), metropolitan area networks (MANs), and mobile communications [38].

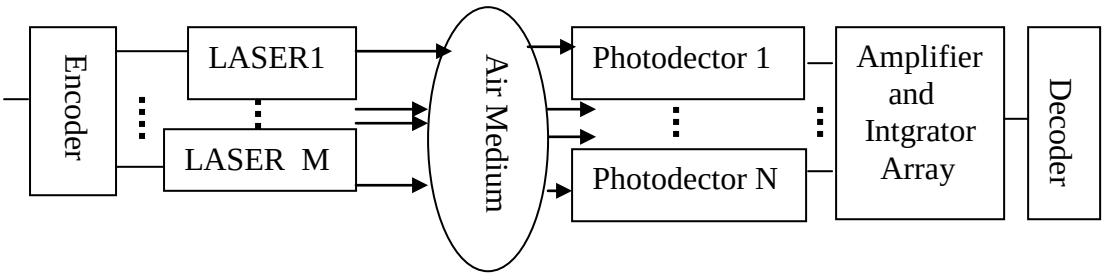

fig: 2.7. Block diagram of MIMO technology

2.8 Limitations of Optical wireless Signal

2.8.1 Scattering

a. Multiple Scattering:

Multiple scattering of waves induces bulk effects such as attenuation and anisotropy that are important in seismology, optics, medical imaging, and other fields involving propagation in disordered media.

b. Homogenous:

Homogenous scattering means scattering produced more than once the same kind of scattering.

c. Mie Scattering

Dielectric spheres are known to scatter electromagnetic radiation if the wavelength of the light is similar to the size of the dielectric sphere. This scattering process was first described theoretically by Mie in 1908. In FTIR spectroscopy, Mie scattering causes a broad sinusoidal oscillation that appears in the baseline of the spectra, which can cause a misrepresentation in the position and intensity of absorption bands.
This Scattering created by such in homogeneities is mainly in the forward direction and called Mie scattering. Mie scattering depending upon the air medium.

d. Scattering Angle:

Scattering Angle means angle between more than one scattering [39].

e. Precise Scattering:

The precise scattering mechanism of light propagating in a medium is dependent on the ratio of the particle radius and the radiation wavelength. When the scattering particles are of the order of magnitude of the radiation wavelength, as is the case for optical wireless communication through fogs and haze at visible and near infrared wavelength [39].

f. Aerosol Scattering:

Aerosol scattering effects caused by rain, snow and fog can also degrade the performance of free space optical communication systems [39].

g. Rayleigh Scattering:

Rayleigh scattering occurs when atmospheric particles are much smaller than the wavelength. Rayleigh occurs primarily off of the gaseous molecules in the atmosphere. Blue light is scattering much more than red light. Rayleigh scattering is responsible for the blueness of the Sky. The effect of Rayleigh scattering on the total attenuation coefficient is very small [40].

h. Atmospheric effect:

Atmospheric turbulence has been studied extensively and various theoretical models have been proposed to describe turbulence induced image degradation and intensity fluctuations. Turbulence induced fading can be reduced substantially by aperture averaging [39].

2.8.2 Attenuation

Free-space laser communication is very similar to fiber optic communication, except that instead of the light being contained within a glass fiber, the light is transmitted through the atmosphere. Since similar optical transmitters and detectors are used for free-space and fiber, similar bandwidth capabilities are achievable. It has also been demonstrated that WDM fiber technologies will also work in free-space, which further increases the bandwidth potential of wireless optical links.6-8,10,11 However, a significant difference between free-space and fiber optic laser transmission is the predictability of the attenuation of laser power in the atmosphere compared to fiber. Fiber optic cables attenuate at a constant predictable rate. Current multimode fiber optic cables attenuate at 2 to 3 dB/km, and single mode fibers attenuate at .5 to .2 dB/km. On the other hand, the atmosphere's attenuation of laser power is quite variable and difficult to predict. Atmospheric attenuation can vary from .2 dB/km in exceptionally clear weather, to 310 dB/km in a very dense UK fog.14,15 These large attenuation values in heavy fog are important because they can reduce the uptime or availability of laser com systems.16 If proposed free-space laser com systems, such as shown in Figure 2.8, are to be used in telecommunication applications, there will be requirements for very high availability. If the system link margin for atmospheric attenuation is 30 dB, then the maximum link range will have to be 100 m or less to always overcome the heaviest 300 dB/km fogs. This is the worst case scenario. In many cases, it will be very difficult to set up lasercom grids between buildings with all them links being less than 100 m in distance. By trading off more link margin and typically less extreme weather, the laser link range requirement can be extended slightly. But to satisfy telecom requirements for availability, the laser links ranges will still have to very short – on the order of less then 500 m, or be backed up by lower data rate microwave or millimeter wave links.

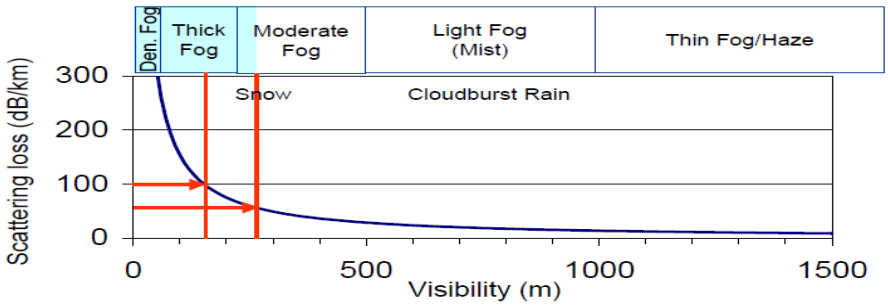

Fig.2.8. The bottom graph shows amount of atmospheric attenuation as a function of visibility. The top shows the weather conditions that correspond to the visibility. Typical laser com systems have 30 to 50 dB of margin at 500 m range which corresponds to handling attenuation up to 60 to 100 dB/km. The primary weather that can cause problems for these short (< 500 m) link ranges is fog and heavy snow.

For these short (<500 m) laser com links, fog and heavy snow are the primary weather conditions which can cause link outages. This is demonstrated in Figure 2.8. The bottom of Figure 2.8 shows a plot of the atmospheric attenuation as a function of the visibility. The technical definition of visibility or visual range is the distance that light decreases to 2% of the original power, or qualitatively, visibility is the distance at which it is just possible to distinguish a dark object against the horizon [40]. There is an obvious inverse relationship between visibility and the amount of attenuation. Also shown above the graph in Figure 2.8 are the descriptive weather conditions that are defined by the corresponding visibilities.14 For example, thick fog is defined as the weather condition where the visibility is between 50 m and 250 m. Typical link margins for atmospheric attenuation can run from 30 dB to 50 dB at 500 m link range for high-end laser com systems. 50 dB of link margin at 500 m corresponds to 100 dB/km of allowable atmospheric attenuation (see arrow at 100 dB/km on the scattering loss axis). This corresponds to weather with a visibility of 150 m (thick fog). Only weather that attenuates worst than 100 dB/km (visibility less than 150 m) will potentially take down the laser link. A system with 30 dB of atmospheric link margin at 500 m range will start to fade in weather which attenuates worse than 60 dB/km or weather with a visibility less then 270 m. In either case, it is fog (dense, thick or moderate) which is the type of weather of primary concern for these short (< 500 m) telecom laser com links. There are also conditions of heavy snow and extreme rain that can attenuate at these high 60 to 100 dB/km levels. In this hypothetical example, losses due to scintillation fades are ignored. But for ranges of 500 m, typical scintillation fade margins are 2 to 5 dB, which is much less than the margins for atmospheric attenuation [41].

2.8.3 Interference

a. Coherence:

A coherent light sources radiation with a continuous succession of waves propagating in phase. This results in a distinct wave front, which is most tangibly discernible when the radiation from two or more a coherent source mixes causing constructive and destructive interference. Coherence interference occurs more than one signal to be place same Phase [42].

b. Incoherence :

Incoherence interference occurs more than one signal to be place different Phase [40].

2.9 FSO System with Diversity

The general diversity setup as shown in Fig. 2.9 has M transmitters and N receivers where M, N ≥ 1and at least one of M or N is greater than 1 [21]. The outputs of the receivers may be combined in any desired way to produce the final observation that is used to make a decision on whether a bit ‘0’ or ‘1’ was sent.

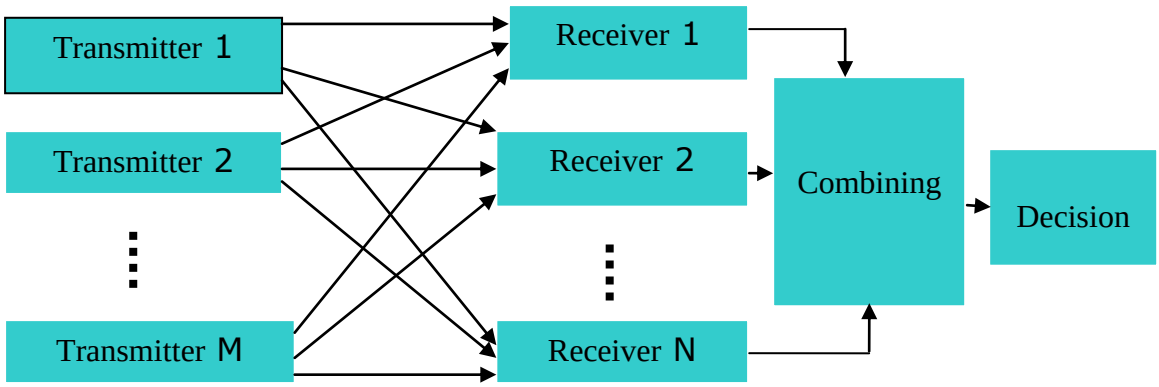

Fig. 2.9. Generic Spatial-diversity transmitter-receiver considering of MIMO.

2.9.1 Receiver diversity with Maximal Ratio Combining

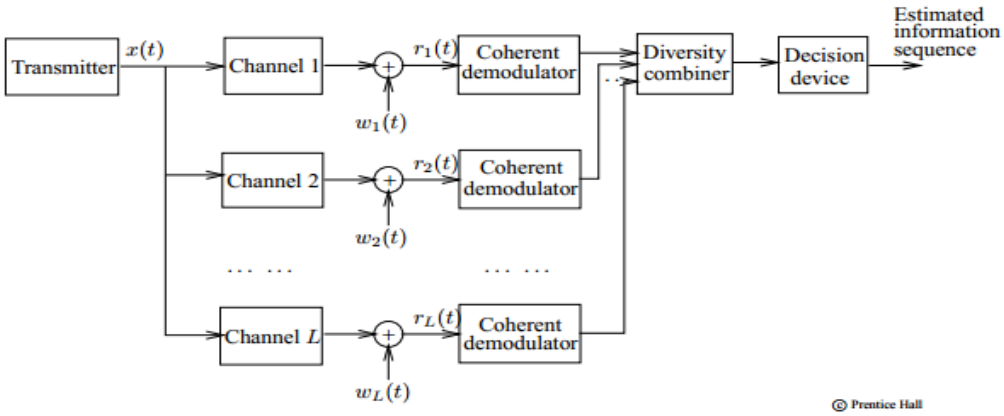

Fig. 2.10. Illustration of diversity with coherent demodulation.

Maximal Ratio combining: This combining technique assumes that the receiver is able to accurately estimate the amplitude fading $\alpha_1(t)$ and carrier phase distortion $\theta_l(t)$ for each diversity channel. With knowledge of the complex channel gains, $\alpha_1(t)\exp[j\,\theta_l(t)]$, l=1, 2,....L, the receiver coherently demodulators the received signal from each branch. The phase distortion $\alpha_1(t)$ of the received signal is removed from the lth branch by multiplying the signal component by exp $[-j\,\theta_l(t)]$. The coherently detected signal is then weighted by the corresponding amplitude gain $\alpha_1(t)$. The weighted received signal from the entire L branch are then summed together and applied to the decision device. Maximal ratio combining achieves the best performance [43].

2.9.2 Receiver Diversity with Equal Gain Combining

Fig. 2.11 shows a FSO system that uses spatial diversity at the receiving end with equal gain combining (EGC) [21]. Each receiver area is A_r/N so that the sum of the areas of the N receivers is the same as the area of the receiver of the no diversity

system. This scaling of area ensures that under no fading, all the described systems have the same received powers. This allows the systems to be compared fairly.

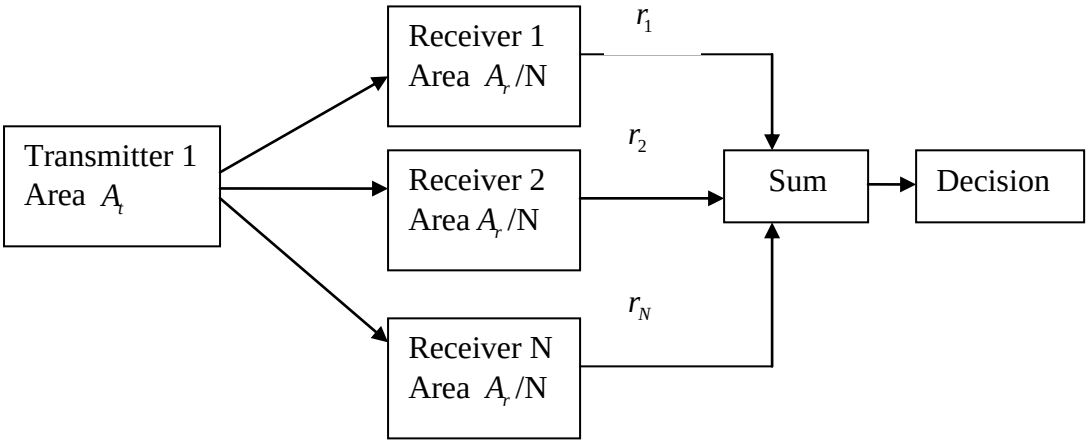

Fig. 2.11. System with receiver diversity and EGC.

2.9.3 Receiver diversity Optimal Combining

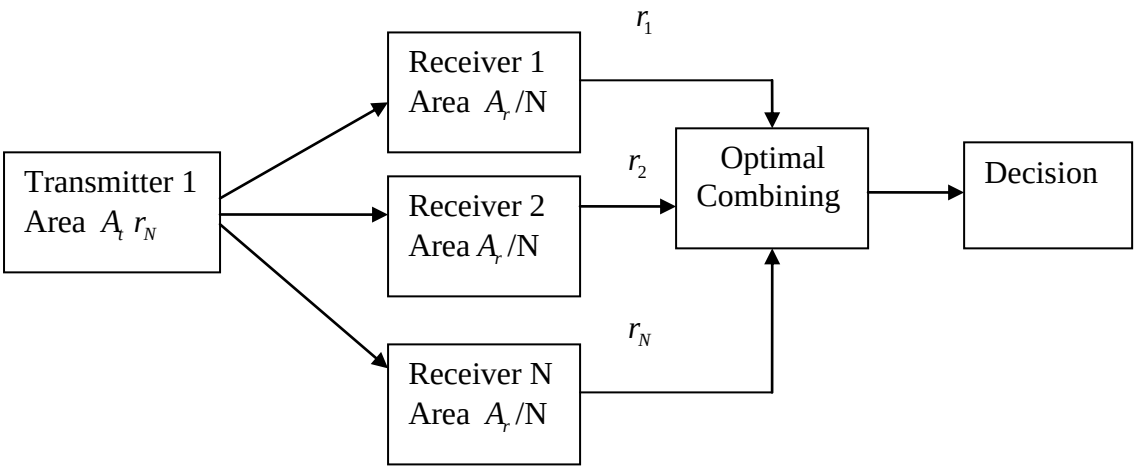

Fig. 2.12. System with receiver diversity and optimal combining

Fig. 2.12 shows a FSO system that uses spatial diversity at the receiving end with optimal combining (OC), also known as maximal ratio combining (MRC) [21]. When MRC Employed, the output of the combiner is a weighted sum of all branches. Branches with high signal-to-noise-ratios are given weights higher than other branches. Here, again each receiver area is A_r/N so that the sum of the areas of the receivers is the same as the area of the receiver of the no diversity system.

Chapter 3

Theoretical analysis

CHAPTER 3

THEORETICAL ANALYSIS OF A FREE SPACE OPTICAL LINK

3.1 System Model

A simple block diagram of a FSO communication link is given in Fig. 3.1 [17]. The transmitter modulates data onto the instantaneous intensity of an optical beam. Here, on-off keying (OOK) is considered which is widely used in practical systems. The received photocurrent signal is related to the incident optical power by the detector responsibility R_d.

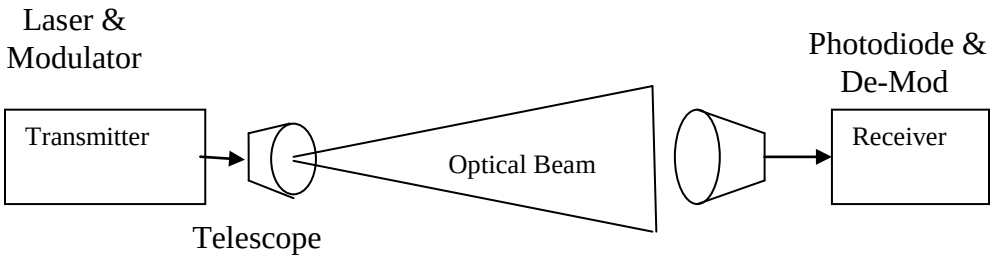

Fig. 3.1. Block diagram of an FSO link.

A detailed block diagram of the transmitter and receiver of a FSO link is shown in Fig. 3.2 [40]. The receiver signal y suffers from intensity fluctuations due to atmospheric turbulence and misalignment, as well as additive noise.

The channel state h models the random attenuation of the propagation channel. Here h arises due to two factors: geometric spread and pointing errors h_p, and atmospheric turbulence h_a. The channel state h can be formulated as

$$h = h_p \, h_a \tag{3.1}$$

The transmitted signal x is either 0 or 2 p_t , where p_t is the average transmitted optical power.

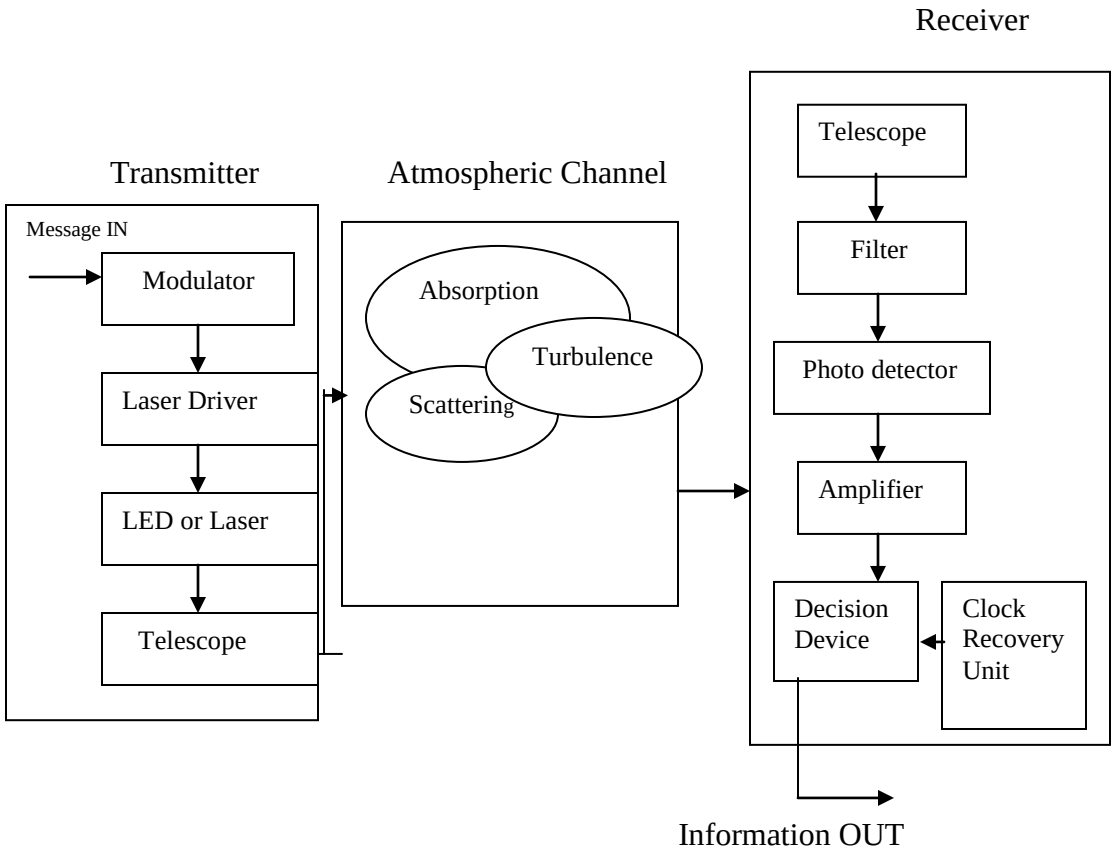

Fig 3.2. Detailed block diagram of OWC System

There are three key functional elements of free-space system OWC System (See Fig. 3.2) the transmitter, the atmospheric channel and the receiver. The transmitter converts the electrical signal into light. The light propagates through the atmosphere to the receiver, which converts the light back into an electrical signal. The transmitter includes a modulator, a laser driver, a LED or laser, and a telescope. The modulator converts bits of information into signals in accordance with the chosen modulation method. The driver provides the power for the laser and stabilizes its performance; it also neutralizes such effects as temperature and aging of the laser or LED. The light sources convert the electrical signal into optic radiation. The telescope aligns the laser LED radiation to a collimated beam and directs it to the receiver. In the atmospheric channel, the signal is attenuated and blurred a as results of absorption, scattering and turbulence. This channel may be the traversed distance between a ground station and a satellite or a path of a few kilometers through the atmosphere between two terrestrial transceivers.
The receiver includes a telescope, filter, photo detector, an amplifier, a decision device, and a clock recovery unit. The telescope collects the incoming radiation and focus it onto filter. The filter removes background radiation and allows only the wavelength of the

signal to pass through it. The photo detector converts the optic radiation into electrical signal, and the amplifier amplifies the electronic signal. The decision unit determines the nature of the bits of information based on the time of arrival and the amplitude of the pulse. The clock recovery unit and synchronizes the data sampling to the decision-making process [40].

3.2 Model of Space Time Block Code (STBC) in a free space optical link

In conventional STBC code [44], in the first bit interval, antenna 1 transmits signal x_1 and antenna 2 transmits signal x_2, in the second bit interval, antenna 1 transmits signal- x_2^*, antenna2 transmits signal x_1^*, they can be described as:

$$\{s_1, s_2\} \rightarrow \begin{bmatrix} x_1 & -x_2^* \\ x_2 & x_1^* \end{bmatrix}$$

where $x_i = \sqrt{2pi}$, p_i is the power of i-th symbol . But in the FSO system, all the signals are the light intensity, they must be real signals. For OOK modulation, the signals can be described as:

s_1=0 ; $0 < t \le T$ light on

s_2=A ; $0 < t \le T$ light off

where 'A' is a positive constant related to the intensity of the light source and T is the signal duration. We can express one of these signal waveforms in terms of the other by

$$s_i = -s_j + A \quad ; \; j \neq i \tag{3.2}$$

The new formation of the transmit symbols can be represented as:

$$\{s_1, s_2\} \rightarrow \begin{bmatrix} x_1 & \bar{x}_2 \\ x_2 & x_1 \end{bmatrix}$$

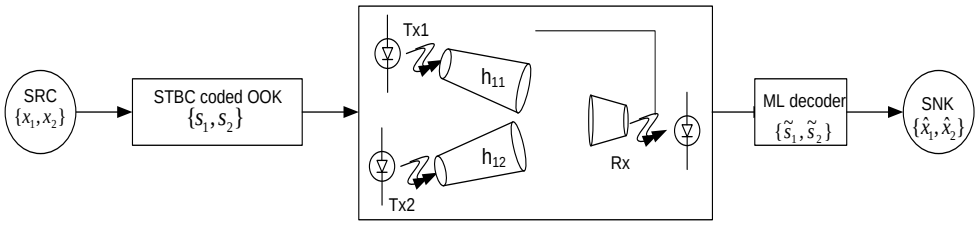

Fig.3.3. Optical communication link with space time block code

For the FSO system we define the complement of a signal x_i as $\overline{x_i}$ where x_i and $\overline{x_i}$ are used for " light on" and "light off" respectively. For example , if $x_i = s_1$ then

$$\overline{x_i} = s_2 = -s_1 + A = -x_1 + A \tag{3.3}$$

Otherwise, if $x_i = s_2$, then

$$\overline{x_i} = s_1 = -s_2 + A = -x_1 + A \tag{3.4}$$

For the FSO system, all the signals must be real signals, based on the above FSO communication model, the received signals in the first and second bit intervals, respectively, are given by ,

$$\begin{bmatrix} y_1 & y_2 \end{bmatrix} = \begin{bmatrix} h_{11} & h_{12} \end{bmatrix} . \begin{bmatrix} x_1 & \bar{x}_2 \\ x_2 & x_1 \end{bmatrix} + \begin{bmatrix} n_1 & n_2 \end{bmatrix} \tag{3.5}$$

*w*here n_1, n_2 are modeled as independent zero-mean Gaussian real random variables with variance σ^2.

3.3 Optical Channel Model

3.3.1 Atmospheric Turbulence Statistical Models:

3.3.1.1 Gamma-Gamma Model:

Many statistical models for the intensity fluctuation through FSO channels have been proposed over the last decades. The log-normal distribution is the most widely used channel model, however its applicability is mainly restricted to weak turbulence conditions [09]. As the strength of turbulence increases, multiple scattering effects must be taken into account. In such cases, log-normal statistical exhibit large deviations compared to experimental data. Furthermore, it has been observed that log-normal probability density function (PDF) underestimates the behavior in the tails as compared with measurement results. Since detection and fade probabilities are primarily based on the tails of the PDF, underestimates this region significantly affects the accuracy of performance analysis [11].

In a recent approach to FSO channel modeling [09], [10], a Gamma-Gamma distribution was used to model atmospheric fading. According to [10], irradiance of the received optical wave is modeled as a product I=xy, Where x arises from large –scale turbulent eddies and y from small scale eddies. It is assumed that x and y are statistically independent random processes. Small-scale contributions to scintillation are associated with turbulent cells smaller than the fresnel zone $R_F = \left(\frac{L}{K}\right)^{1/2}$ or the coherence radius ρ_o, whichever is smaller. Large-scale fluctuation in the irradiance is generated by turbulent cells larger than that of the first fresnel zone or the scattering disk L/k ρ_o whichever is larger. Under strong fluctuation condition, spatial cells having size between those of the

coherence radius and the scattering disk contribute little to scintillation. That is, because of the loss of spatial coherence, only the very largest cells nearer to the transmitter have any focusing effect on the illumination of small diffractive cells nearer to the receiver, and eventually even these large cells cannot focus or defocus. When this loss of coherence happens, the illumination of the small cells is (statistically) evenly distributed and the fluctuation of the propagating wave are just due to random interference of large number of diffraction scattering of the small cells.

Each of the large and small scale eddies follow the gamma distribution, i.e.

$$p_x(x) = \frac{\alpha(\alpha x)^{\alpha-1}}{\Gamma(\alpha)} \exp(-\alpha x), x > 0, \alpha > 0 \tag{3.6}$$

$$p_y(y) = \frac{\beta(\beta y)^{\beta-1}}{\Gamma(\beta)} \exp(-\beta y), y > 0, \beta > 0 \tag{3.7}$$

This leads to the gamma-gamma pdf, i.e

$$f(I) = \frac{2(\alpha\beta)^{(\alpha+\beta)/2}}{\Gamma(\alpha)\Gamma\beta} I^{(\alpha+\beta)/2-1} k_{(\alpha-\beta)} 2\sqrt{\alpha\beta I}, I > 0 \tag{3.8}$$

Where $k_a(.)$ is the modified bessel's function of the second kind of order α. The positive parameter α represents the effective number of large-scale cells of the scattering process and β similarly represents the effective number of small–scale cells. When optical turbulence is weak, the effective number of scale sizes smaller and larger than the first fresnel zone is large, resulting in $\alpha >> 1$ and $\beta >> 1$. Assuming spherical wave propagation, these parameters can be directly related to atmospheric conditions according to [10], [11].

$$\alpha = \left[\exp\left(\frac{.49x^2}{(1+0.18d^2+0.56x^{12/15})^{7/6}}\right) - 1 \right]^{-1} \tag{3.9}$$

$$\beta = \left[\exp\left(\frac{.51x^2(1+0.69x^{12/15})^{-5/6}}{(1+0.9d^2+0.62d^2x^{12/15})^{5/6}}\right) - 1 \right]^{-1} \tag{3.10}$$

Where $x^2 = .5C_n^2 k^{7/6} L^{11/6}$ and $d = (KD^2/4L)^{1/2}$. Here $k = 2\pi/\lambda$ is the optical wave number λ is the wavelength, D is the diameter of the receiver collecting lens aperture and L is the link distance in meters. C_n^2 stands for the index of refraction structure parameter and is altitude dependent [09]. where $C_n^2 = 79.06\left(\frac{P}{T^2}\right) * C_\theta^2 * 10^{-6}$, P is the pressure, T is the temperature and C_θ^2 is the structure function for potential temperature [45].

For Weak turbulence values [46] $C_n^2 \le 10^{-14} m^{-2/3}$

For Moderate turbulence values [46] $C_n^2 = 10^{-14} m^{-2/3}$

For Strong turbulence values [46] $C_n^2 \geq 10^{-14} m^{-2/3}$

3.3.1.2 Lognormal Turbulence Model

The atmospheric turbulence impairs the performance of an FSO link by causing the received optical signal to vary randomly thus giving rise to signal fading. The fading strength depends on the link length, the wavelength of the optical radiation and the refractive index structure parameter c_n^2 of the channel. The log-normal distribution is generally used to model the fading associated with the weak atmospheric turbulence regime [47]. This model is mathematically tractable and it is characterized by the variance σ_1^2. The turbulence induced fading is termed weak when σ_1^2 <1.2 and this defines the limit of validity of the log-normal model [47]. Beyond the weak turbulence regime, other models like the gamma-gamma [47] and the negative exponential [47] will have to be considered. The variance σ_1^2 can be calculated as [47]:

$$\sigma_1^2 = 1.23\, c_n^2 (\sqrt[6]{k^7 L^{11}}) \tag{3.11}$$

where L is the propagation distance and k is the wave number. The log-normal models assumes the log intensity of the laser light traversing the turbulent atmosphere to be normally distributed with a mean value of $\sigma_1^2/2$. Thus, the probability density function of the received irradiance is given by [47]:

$$f_I(I) = \frac{1}{I\sqrt{2\pi\sigma_l^2}} \exp\{-\frac{[\ln(I/I_0 + \sigma_l^2/2)]^2}{2\sigma_l^2}\} dI \tag{3.12}$$

where I represent the irradiance at the receiver including turbulence effect and I_0 is the average signal irradiance without turbulence effect.

3.4 Derivation of BER Expressions

3.4.1 SISO FSO Link

The transmitted optical signal can be represented as:

$$S(t) = \sum_{-\infty}^{\infty} a_k\, p(t - kT) * \sqrt{2P_T}\, e^{j\omega_c t} \tag{3.13}$$

where,

a_k = Data bit (0,1), p(t) = Pulse Shape, P_T = Transmitter Power

ω_c = Carrier frequency

We consider intensity modulation/direct detection (IM/DD) links using on-off keying (OOK). In most practical systems, the receiver signal-to-noise ratio (SNR) is limited by

shot noise caused by ambient light much stronger than the desired signal and/ or by thermal noise in the electronics following the photo detector. In this case, the noise can usually be modeled to high accuracy as additive white Gaussian noise that is statistically independent of the desired signal [47].

$$x(t) = R_d \left|s(t)\right|^2 + n(t)$$
$$= R_d \, \mathrm{I(t)+n(t)} \tag{3.14}$$

where I(t) is the received optical intensity with turbulence given by

$$I(t) = I_0 * h(t) \tag{3.15}$$

h(t) represents the intensity fluctuation due to atmospheric turbulence. R_d is the photodetector responsibility and n(t) represents AWGN (Additive White Gaussian Noise) with variance $\sigma_n^2 = \sigma_{thermal}^2 + \sigma_{Shot}^2$, $\sigma_{thermal}^2$ represents the thermal noise variance, σ_{Shot}^2 represents the shot noise variance.

At a given value of h(t)=h and $I_0 = P_s$, the conditional signal to noise ratio (SNR) conditioned on a given value of h, at the receiver output is given by

$$\text{SNR (h)} = \frac{(R_d P_s)^2 * h^2}{\sigma_n^2} \tag{3.16}$$

where,

$$\sigma_{shot}^2 = 2eB(P_s + p_b)R_d$$

$$\sigma_{th}^2 = \frac{4kTB}{R_L}$$

where e is the electronic charge, B is the Bandwidth of receiver filter, k is the Boltzmann's constant, T is the receiver noise temperature in degree Kelvin and R_L is the receiver load resistance.

For OOK modulation, the bit error rate can be calculated as:

$$p_b(e) = p(1)(e/1) + p(0)\,p(e/0) \tag{3.17}$$

where (p1) and p(0) are probabilities of sending a '1' and '0' respectively. p(e/1) and p(e/0) are the conditional error probabilities when the transmitted bit is '1' and '0'. Considering that p(1) =P(0)=1/2 and p (e/1)=p(e/0), it can be shown that conditioned on a given value of h, the conditional BER is given by [48]:

$$p_b(e|h) = Q\left[\frac{\sqrt{2}R_d P_s h}{\sigma_n}\right] = Q\left[\sqrt{2(SNR}\right] \tag{3.18}$$

The average BER, $p_b(e)$ can be obtained by averaging (3.18) over the pdf of h as:

$$p_b(e) = \int_0^\infty f_h(h)\, p_b(e|h)dh \tag{3.19}$$

$f_h(h)$ is given by (3.12).

3.4.2. Receiver Diversity (Single Input Multiple Output, SIMO)

Consider the transmission of a digital modulated signal x (t) over flat slow Rayleigh fading channel using coherent demodulation with Nth order diversity. The received signal component from Nth diversity channel is [49]

$$r_n(t) = \alpha_n(t)\exp[j\theta_n(t)]x(t) + u(t)$$

where, n = 1, 2, 3……., N

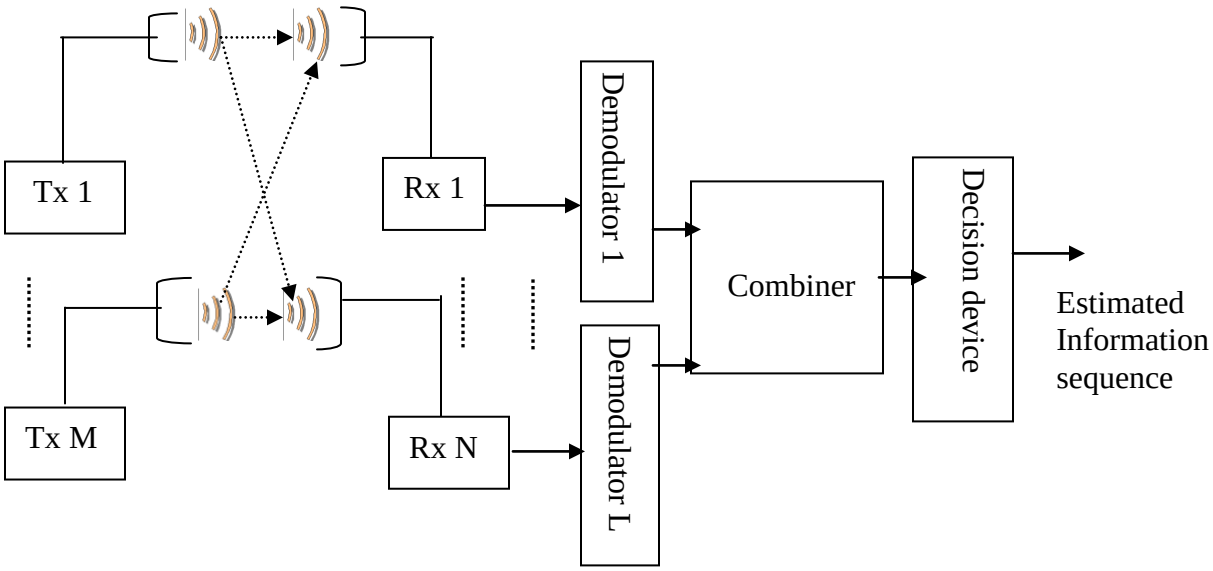

Fig. 3.4. Diversity reception with maximal ratio combining

The decision variable for the kth transmitted symbol can be represented by

$$\begin{aligned} r_k(t) &= \sum_{n=1}^{N} \alpha_{nk} \exp(-j\theta_{nk})[\alpha_{nk} \exp(j\theta_{nk})x(t) + n_{nk}] \\ &= \left[\sum_{n=1}^{N} \alpha_{nk}^2\right] x(t) + \left[\sum_{n=1}^{N} \alpha_{nk} \exp(-j\theta_{nk}) n_{nk}\right] \\ &= g_k x(t) + n_k \end{aligned} \tag{3.20}$$

where,

$$g_k = \sum_{n=1}^{N} \alpha_{nk}^2$$

and

$$n_k = \sum_{n=1}^{N} \alpha_{nk} \exp(-j\theta_{nk}) n_{nk}$$

We consider, $x(t) = \sqrt{E_b}$ for symbol "1" and $x(t) = -\sqrt{E_b}$ for symbol "0". The SNR per bit at the output of the combiner for the kth symbol is then

$$\gamma_k = \frac{[g_k x(t)]^2}{2\sigma_{k,n}^2} = \frac{\left[\sum_{n=1}^{N} \alpha_{nk}^2 x(t)\right]^2}{N_0 \sum_{n=1}^{N} \alpha_{nk}^2} = \frac{E_b}{N_0} \sum_{n=1}^{N} \alpha_{nk}^2 \tag{3.21}$$

For a Rayleigh fading, the probability density function of γ is given by [48]

$$f_\gamma(x) = \frac{x^{N-1} \exp(-x/\Gamma_c)}{(N-1)!\Gamma_c^N} \tag{3.22}$$

Consider maximal ratio combining gain, the probability of bit error over Rayleigh fading channel can be expressed as [49].

$$P_b(e/h) = [0.5(1-\mu)]^N \sum_{n=0}^{N-1} \left(\frac{(N-1+n)!}{n!(N-1)!}\right) [0.5(1-\mu)]^N \tag{3.23}$$

where,

$$\mu = \sqrt{\frac{\Gamma_c}{1+\Gamma_c}}$$

here $\Gamma_c = \sqrt{SNR(h)}$

The average BER for a SIMO optical link can be obtained as:

$$P_{b,\,SIMO} = \int f_h(h).P_b(e/h)dh \tag{3.24}$$

3.4.3 FSO link With Diversity (MIMO FSO)

Assuming on off keying (OOK), the received signal at the nth receiver is given by [24]

$$r_n = R_d X \sum_{m=1}^{M} h_{mn} + \upsilon_n \text{ , n=1,... N} \tag{3.25}$$

where the transmitted signal, $x \in \{0, 2P_t\}$, P_T being the average transmitted optical power and h_{mn} denotes the fading coefficient from the m[th] transmitter to the n[th] receiver. A schematic block diagram of such a system is shown in Fig. 3.4

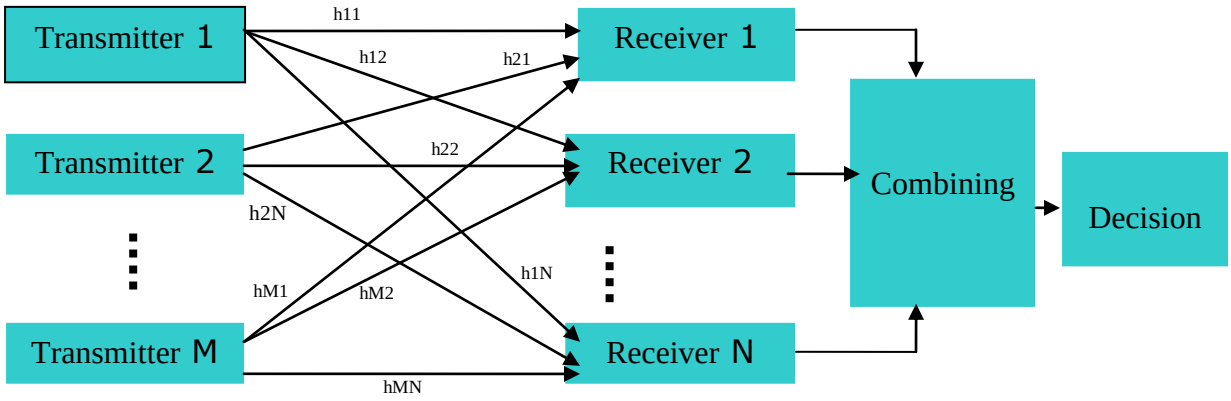

Fig. 3.5. Setup of a MIMO FSO Link

Following from [25], we obtain the probability distribution function of h_{mn} including the effect of pointing error as:

$$f_{h_{mn}}(h_{mn}; w_z) = \frac{2\gamma^2(\alpha_{mn}+\beta_{mn})^{(\alpha_{mn}+\beta_{mn})^2}}{(A_0)^{\gamma^2}\Gamma(\alpha_{mn})(\Gamma\beta_{mn})} h^{\gamma^2-1} \int_{h/A_0}^{\infty} h_a^{(\alpha_{mn}+\beta_{mn})/2-1-\gamma^2} K_{\alpha_{mn}-\beta_{mn}}\left(2\sqrt{\alpha_{mn}\beta_{mn}h_a}\right) dh_a \quad (3.26)$$

The optimum decision metric for OOK is given by [25],

$$p(r/1, h_{mn}) \underset{<_0}{\overset{>1}{}} p(r|0, h_{mn}) \quad (3.27)$$

where r = $(r_1, r_2, ...r_n)$ is the received signal vector and the conditional probabilities are

$$p(r|1, h_{mn}) = \frac{\exp\left(-\frac{1}{2\sigma_n^2}\sum_{n=1}^{N}(r_n - 2\sqrt{2}R_d P_t \sum_{m=1}^{M} h_{mn})^2\right)}{(2\pi\sigma_n^2)^{N/2}} \quad (3.28)$$

and

$$p(r/0,h_{mn})\frac{\exp\left(-\frac{1}{2\sigma_n^2}\sum_{n=1}^{N}r_n^2\right)}{(2\pi\sigma_n^2)^{N/2}} \tag{3.29}$$

For the '1' and 0 states, respectively. By putting (3.28) and (3.29) in (3.27) as was done in [24] and dropping out the common terms, the result is

$$-\sum_{n=1}^{N}(r_n-\sum_{m=1}^{m=1}2\sqrt{2}R_dP_th_{mn})^{2\overset{1}{<_0}}-\sum_{n=1}^{N}(r_n)^2 \tag{3.30}$$

This equation can be further simplified as

$$\sum_{n=1}^{N}\sum_{m=1}^{M}2\sqrt{2}R_dP_th_{mn}r_n\overset{1}{<_0}\frac{1}{2}\sum_{n=1}^{N}\left(\sum_{m=1}^{M}2\sqrt{2}R_dP_th_{mn}\right)^2 \tag{3.31}$$

The conditional bit error rates are given below.

$$p_b\left(e\middle|0,h_{mn}\right)=p\left[\sum_{n=1}^{N}\sum_{m=1}^{M}2\sqrt{2}R_dP_th_{mn}r_n>\frac{1}{2}\sum_{n=1}^{N}\left(\sum_{m=1}^{M}2\sqrt{2}R_dP_th_{mn}\right)^2\middle|r_n=v_n\right]$$

$$=p\left[\sum_{n=1}^{N}\sum_{m=1}^{M}2\sqrt{2}R_dP_th_{mn}v_n\frac{1}{2}\sum_{n=1}^{N}\left(\sum_{m=1}^{M}2\sqrt{2}R_dP_th_{mn}\right)^2\right]$$

$$=Q\left(\frac{1}{2\sigma_n}\sqrt{\left[\sum_{n=1}^{N}\left(\sum_{m=1}^{M}2\sqrt{2}R_dP_th_{mn}\right)^2\right]}\right) \tag{3.32}$$

$$p_b\left(e\middle|1,h_{mn}\right)=p\left[\sum_{n=1}^{N}\sum_{m=1}^{M}2\sqrt{2}R_dP_th_{mn}r_n<\frac{1}{2}\sum_{n=1}^{N}(2\sqrt{2}R_dP_t\sum_{m=1}^{M}h_{mn})^2\middle|r_n=\sum_{m=1}^{M}2\sqrt{2}R_dP_th_{mn}+v_n\right]$$

$$=p\left[2\sum_{n=1}^{N}\sum_{m=1}^{M}2\sqrt{2}R_dP_th_{mn}(R_dP_t\sum_{m=1}^{M}h_{mn}+v_n)<\sum_{n=1}^{N}(2\sqrt{2}R_dP_t\sum_{m=1}^{M}h_{mn})^2\right]$$

$$=Q\left(\frac{1}{2\sigma_n}\sqrt{\sum_{n=1}^{N}(2\sqrt{2}R_dP_t\sum_{m=1}^{M}h_{mn})^2}\right) \tag{3.33}$$

Averaging over the fading coefficients, the BER of a MIMO system is obtained as [47]:

$$BER = \int_{h_{mn}} f_{h_{mn}}(h_{mn}) Q[\frac{\sqrt{2}}{\sigma_n MN} \sqrt{\sum_{n=1}^{N} (\sum_{m=1}^{M} R_d P_t h_{mn})^2}] dh_{mn} \quad (3.34)$$

where $f_{h_{mn}}(h_{mn})$ is the joint pdf of vector $h = (h_{11}, h_{12}....., h_{MN})$ of length MN. The average in (3.30) can be calculated through multi-dimensional numerical integration. In order to fairly compare the scaling factor MIMO links with the SISO one, the factor M is used in (3.29) to ensure the total transmit power in the MIMO system is the same as the power of SISO system [25]. Moreover, the factor N is used so that the total receiver area of the MIMO link is the same as the receiver area of the SISO link.

3.4.4 Transmitter Diversity (Multiple Input Single Output, MISO)

When only transmit diversity is used with single receiver, i.e. N=1, the bit error rate (BER) of a MISO system can be written as [48]:

$$P_b BER_{,MISO} = \int_{h_{mn}} f_{h_{mn}}(h_{mn}) Q(\frac{\sqrt{2}}{\sigma_n M} \sum_{m=1}^{M} R_d P_t h_m) dh_{mn} \quad (3.35)$$

Chapter 4

Results and Discussion

CHAPTER 4

RESULT AND DISCUSSION

4.1 Introduction

This chapter represents the results obtained from computation on the model of FSO wireless communication system considering the SISO, SIMO, MISO, MIMO system described in chapter-3. Results are evaluated numerically and degradation of system performance due to channel impairments is determined in terms of power penalty due to atmospheric turbulence at a given BER with respect to without turbulence. The system parameters used for numerical computations are shown in table 4.1

Table: 4.1: System Parameters

Parameter	Value
Transmission Rate	1 Gbps
Responsibility of photodector (R_d)	0.8
Noise standard deviation	0.125-1.325
Temperature	300 Kelvin
Electron charge	1.6*10^-19 coulombs
Boltzsmann constant	1.38*10^-23 m^2 kg s^{-2} K^{-1}
Load resistance	50 ohms

4.2 Performance Results of SISO System

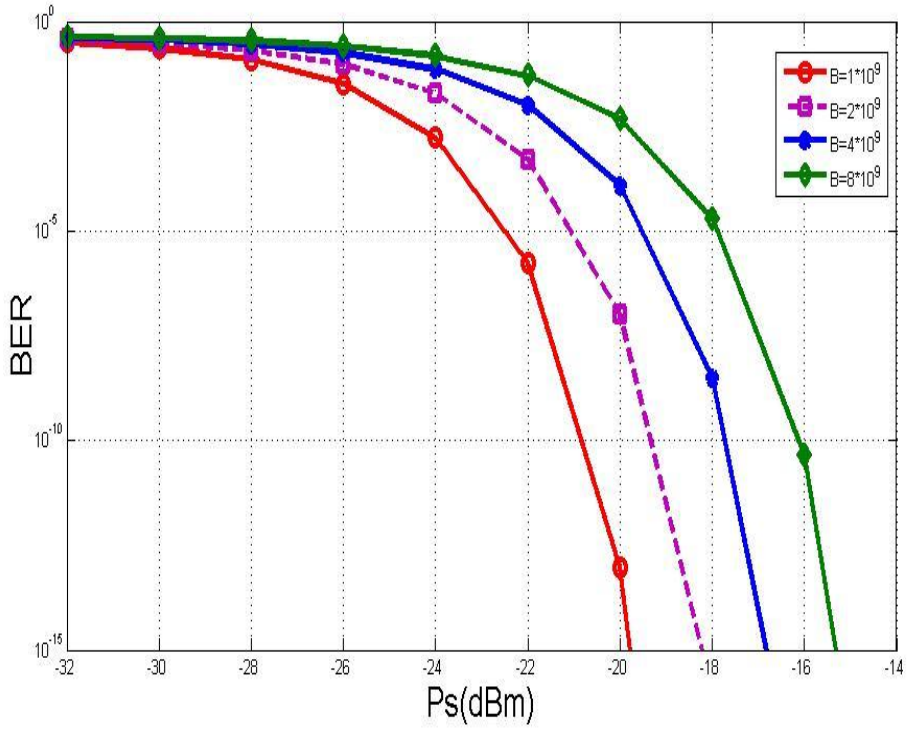

Fig 4.1. BER versus Optical received power for a SISO FSO link without turbulence

Fig. 4.1 shows that BER vs. P_s without turbulence for different bandwidth. From the curves, it is seen that the BER increases with increases the bandwidth. At the P_s = -22dBm, the BER are approximately 10^{-05} for Bandwidth 1GHz and 10^{-03} for Bandwidth 2GHz respectively. The received power increases when the bandwidth increases.

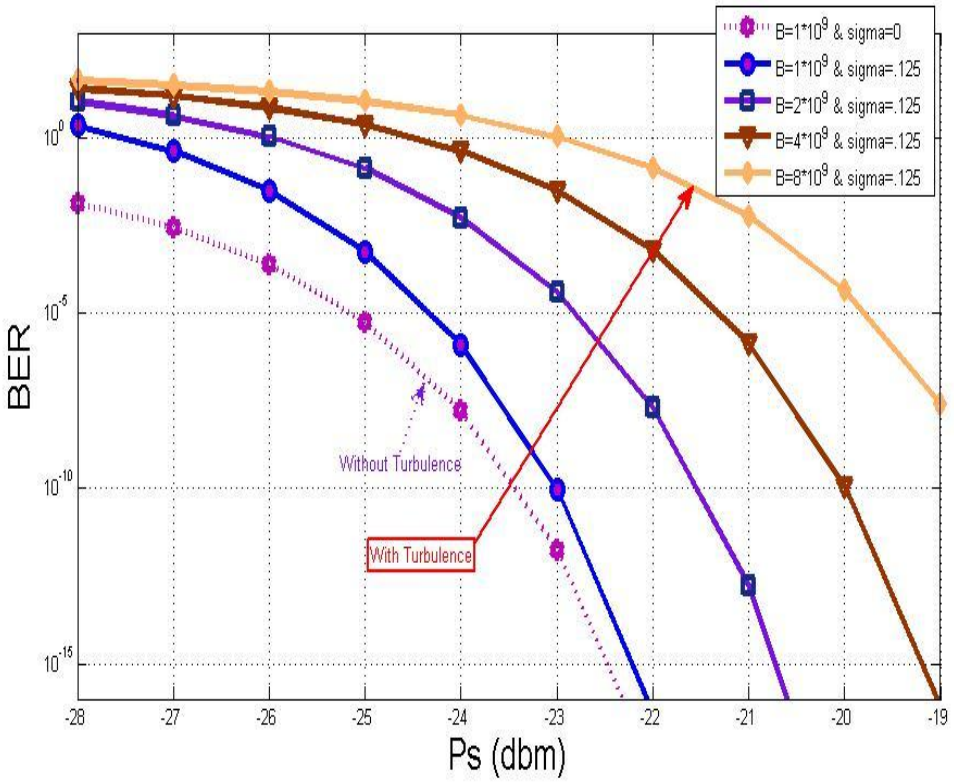

Fig 4.2. BER versus received optical power for a SISO FSO link with turbulence

BER vs. P_s with turbulence for different bandwidth and standard deviation of turbulence sigma is shown in Fig. 4.2. When sigma is equal to zero then it is without turbulence. For turbulence, the value of sigma is 0.125. It is also seen that the BER increases with increase in bandwidth. At the P_s = - 24dBm, the BER are approximately 10^{-06} when Bandwidth is 1GHz and BER= 10^{-02} when Bandwidth is 2 GHz respectively. Further, the required received optical power increases with increase in bandwidth. Thus the system suffers power penalty due to turbulence which is higher at higher bandwidth.

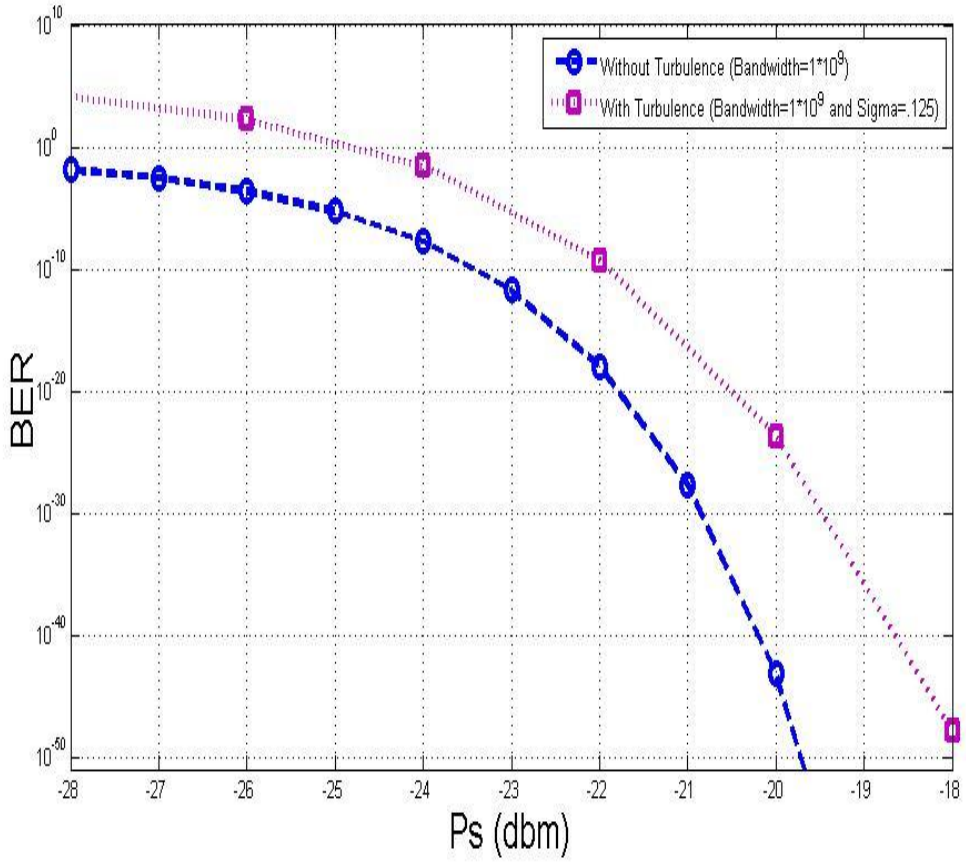

Fig 4.3. Comparison between without and with turbulence

Fig. 4.3 depicts the comparison of without and with turbulence for same bandwidth. From the curves, it is seen that the BER of with turbulence is higher than without turbulence. At the P_s = - 22dBm, the BER are approximately 10^{-19} (without turbulence) and 10^{-09} (with turbulence) respectively. Further, There is increase in required received optical power at a given BER $=10^{-10}$ which is the power penalty due to turbulence at a given bandwidth.

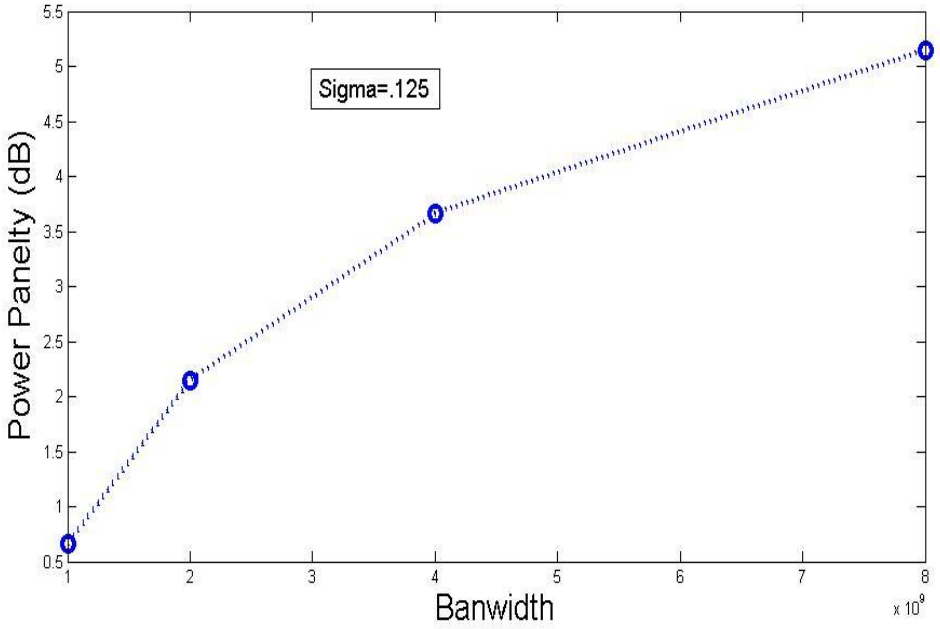

Fig 4.4. Power penalty versus Bandwidth for SISO FSO link.

The plots of power penalty vs. Bandwidth are shown in Fig. 4.4. For sigma= 0.125. It is seen that as the Bandwidth increases, the power penalty increases due to increase effect of turbulence. At the Bandwidth 4 GHz, the power penalty is approximately 3.5 dB and is higher at higher bandwidth.

4.3 Performance Results of SIMO System

The BER performance results for SIMO optical link are evaluated numerically and the power penalty due to atmospheric turbulence at different bandwidth are determined at a BER=10^{-09} .

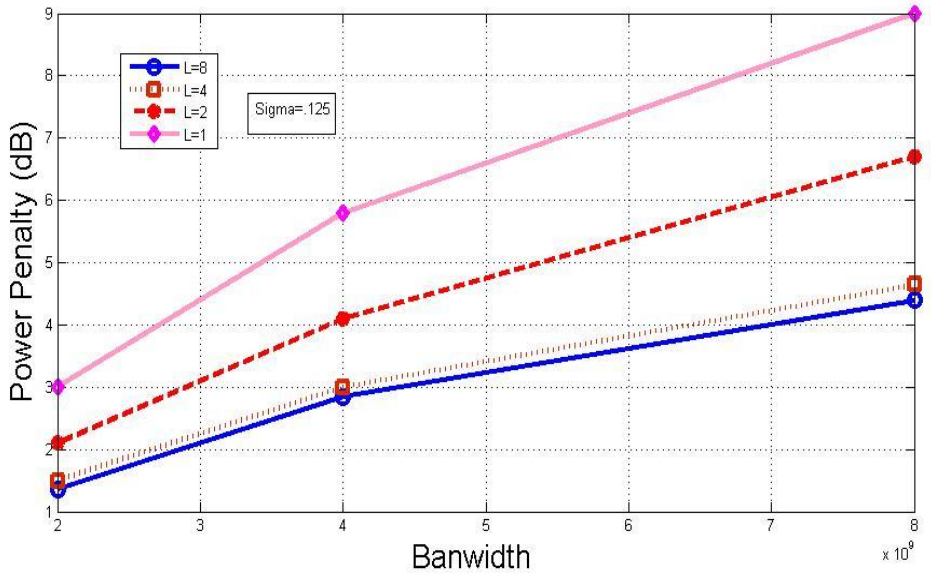

Fig 4.5. Power penalty versus Bandwidth for SIMO FSO link

The plots of the power penalty as a function of bandwidth are shown in figure 4.5 for different number of optical receiver L and considering sigma=.125.

From the graph, bandwidth increases, power penalty also increases. For higher number of optical receivers, power penalty is lower. At the Bandwidth 4 GHz, the power penalty are approximately (L means receiver) 3dB for L = 8 and 5.9 dB for L = 2. Thus as the number of optical receiver increases, there is improvement in overall system performance which is depicted in fig. 4.8.

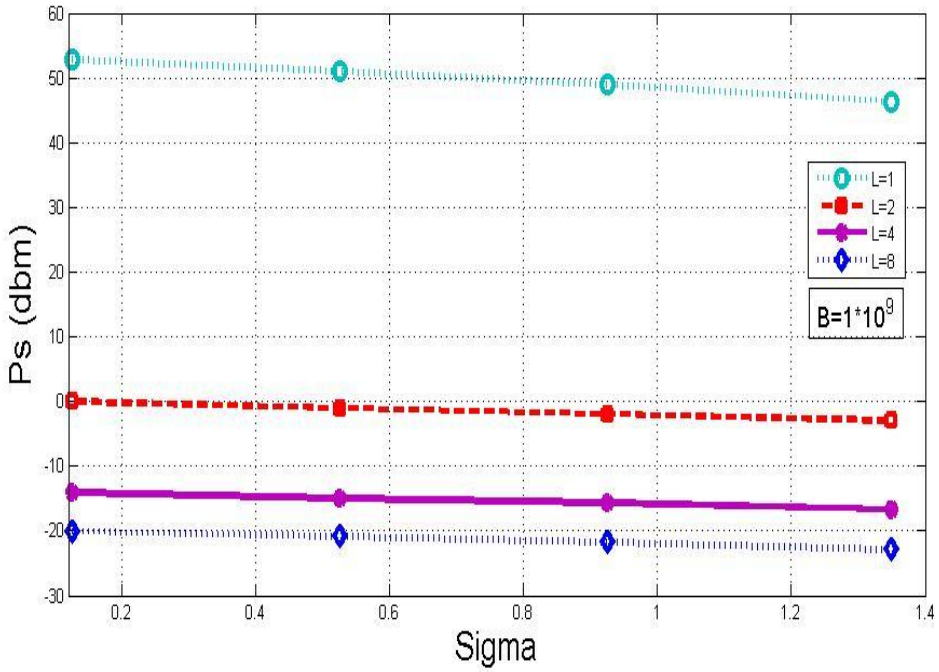

Fig 4.6. Received optical power versus Sigma for SIMO FSO link.

The plots of receiver sensitivity in terms of received optical power P_s (dBm) are shown in figure 4.6 as a function of standard deviation of turbulence, sigma for different number of receivers. It is noticed that there are improvement in receiver sensitivity at a given sigma with increase in number of receiver. Further, there is slight improvement in receiver performance with increase in sigma.

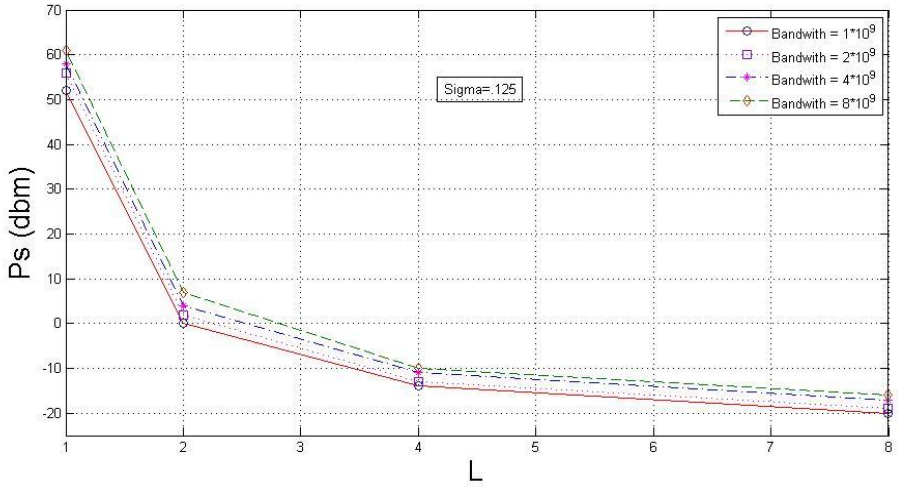

Fig 4.7. Received optical power versus receiving antenna

The plots of receiver sensitivity versus number of receivers are shown in fig. 4.7 for sigma =.125 for different bandwidth. As seen from the plots there are significant reduction in required received optical power as the number of receivers is increased.

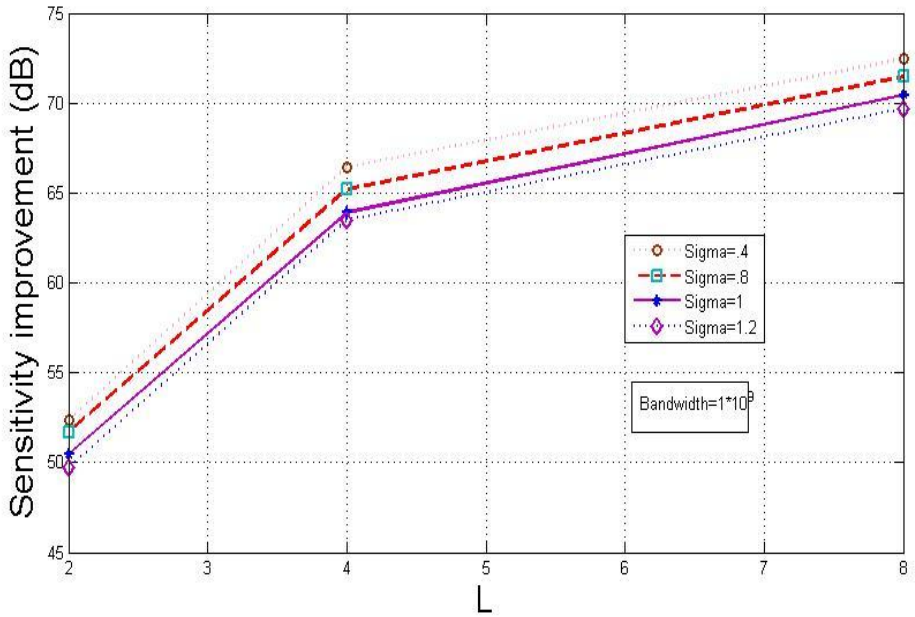

Fig 4.8: Receiver Sensitivity improvement versus number of receiver for SIMO FSO link.

Fig. 4.8 shows the receiver sensitivity improvement vs. number receiver for different sigma at Bandwidth 1 GHz. It is found that there is significant improvement in receiver sensitivity due to diversity in number of receiver.

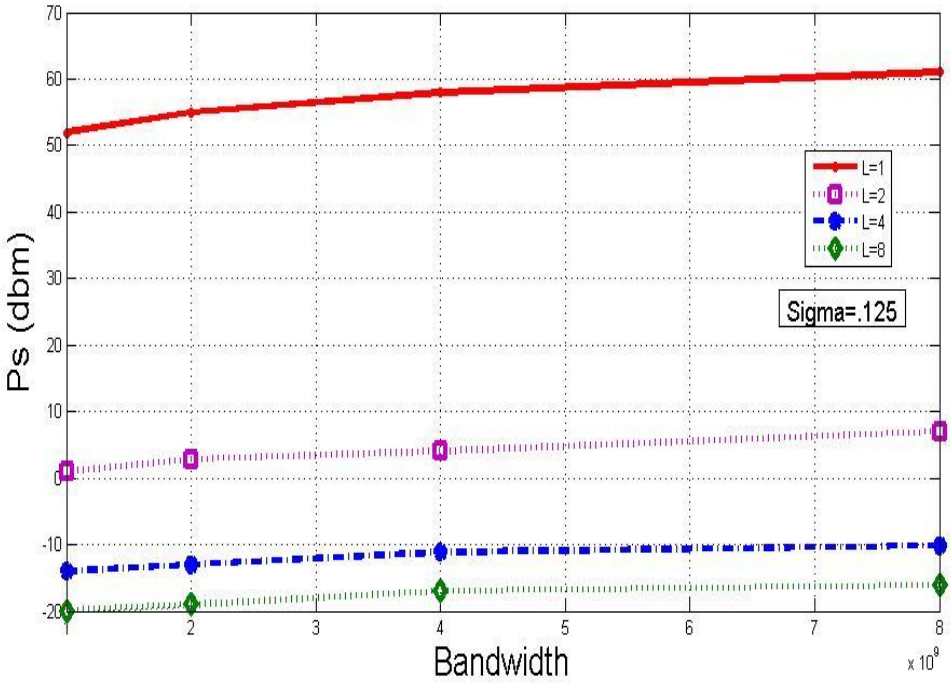

Fig 4.9. Receiver sensitivity at BER = 10^{-09} versus bandwidth for SIMO FSO link.

The variation of receiver sensitivity at BER = 10^{-09} with bandwidth is shown in fig. 4.9 for different number of receiver. It is seen that there is degradation in receiver perform due to increased effect of atmospheric turbulence at higher bandwidth.

4.4 Performance Results of MISO System

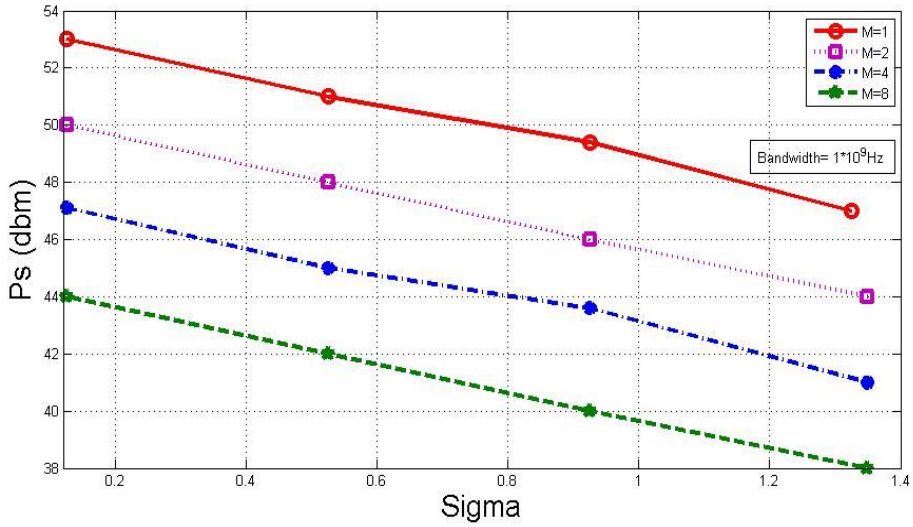

Fig 4.10: Optical received power versus Sigma for MISO FSO link

Fig. 4.10 shows that P_s vs. Sigma for number of transmitter antenna. For turbulence, the bandwidth has used 1GHz. From the graph, transmitted power decreases with increases number of transmitter. For the higher number of transmitting antenna, transmitted power is lower. When the sigma increases, the transmitted power

decreases. At the sigma = 0.6, the transmitted power are approximately (M means Transmitter) 41.5 (M = 8) and 47.5 (M = 2) dB. When the transmitting antenna increases it has improved the system performance.

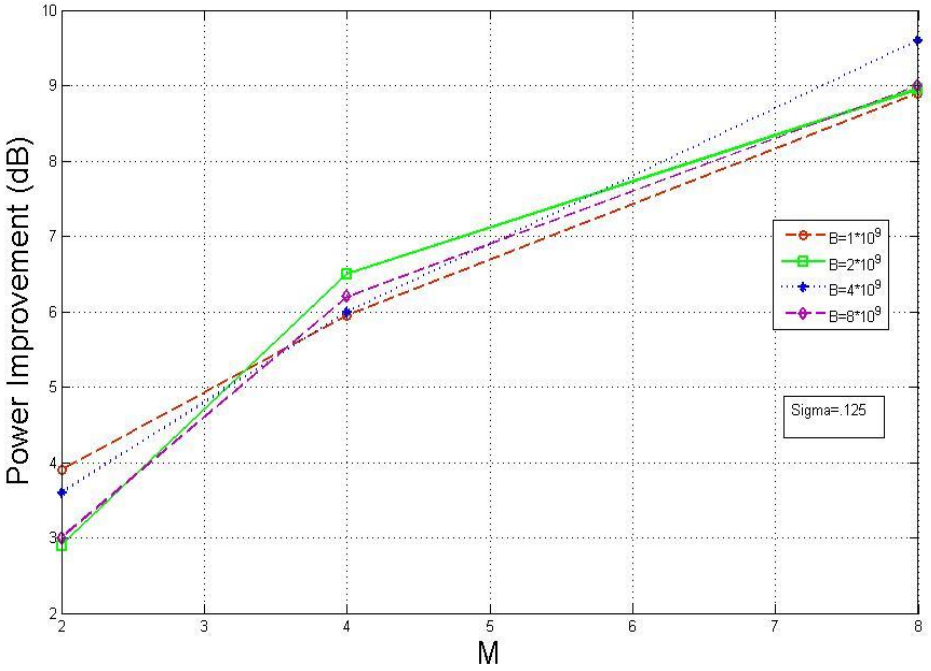

Fig 4.11. Power improvement versus transmitted antenna for MISO FSO link

Fig. 4.11 depicts that Power improvement vs. transmitted antenna for different bandwidth. For turbulence, the sigma has used 0.125. From the graph, power has improved due to the number of transmitter are increased.

4.5 Performance Results of MIMO System

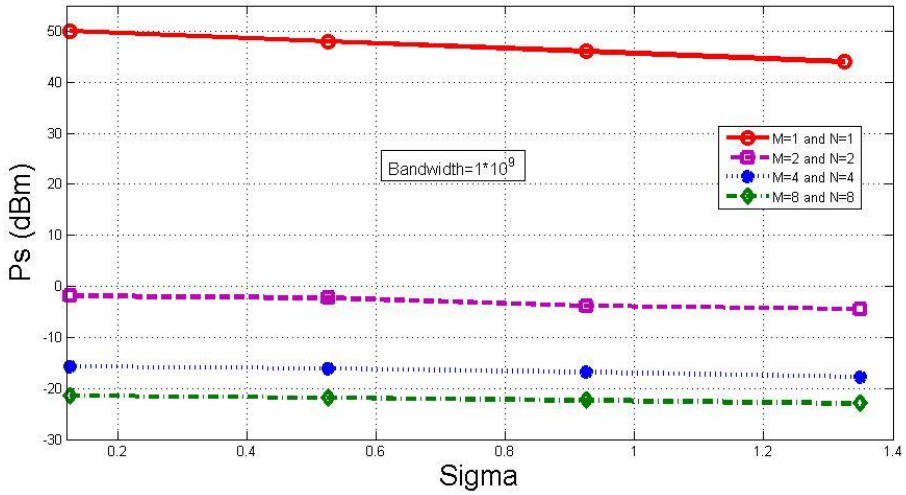

Fig 4.12: Received optical power versus Sigma for MIMO FSO link

Received power vs. sigma is shown in Fig. 4.12. For turbulence, the bandwidth has used 1GHz. It is also seen that the number of transmitter and receiver has increased, the power penalty has also decreased. At the sigma = 0.6, the transmitted power penalty are approximately 48 dBm for M = 1 and N = 1 and -19 dBm for M = 8 and N = 8.

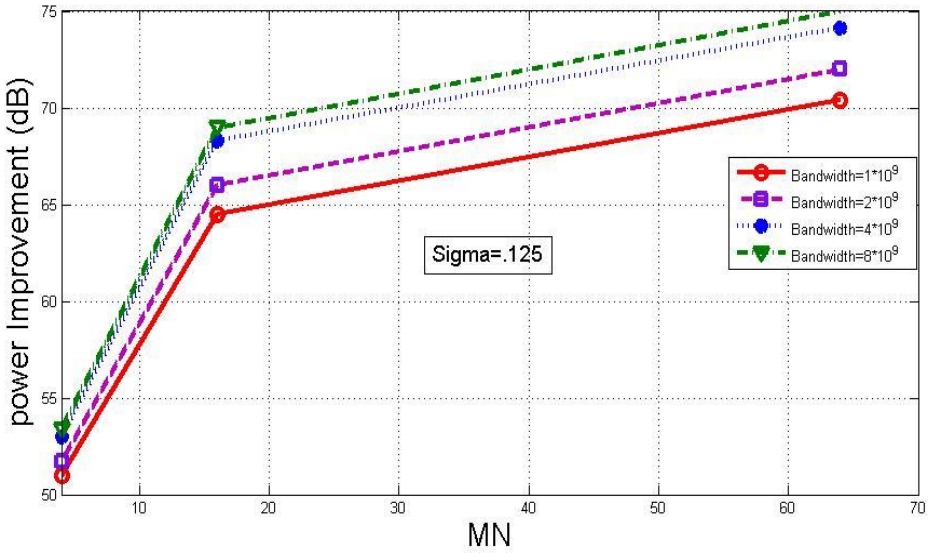

Fig 4.13. Power improvement versus multiplication of the no. of transmitters and receivers for MIMO FSO link

Fig. 4.13 shows that Power improvement vs. transmitter and receiver for different bandwidth. For turbulence, the sigma has used 0.125. From the graph, bandwidth increases with improves power. For the higher number of transmitting and receiving antenna, power has the better than others. When the transmitting and receiving antenna increases it has improved the system performance.

4.6 Comparison between Previous work and our work

Comparing between previous work and our work is bellow

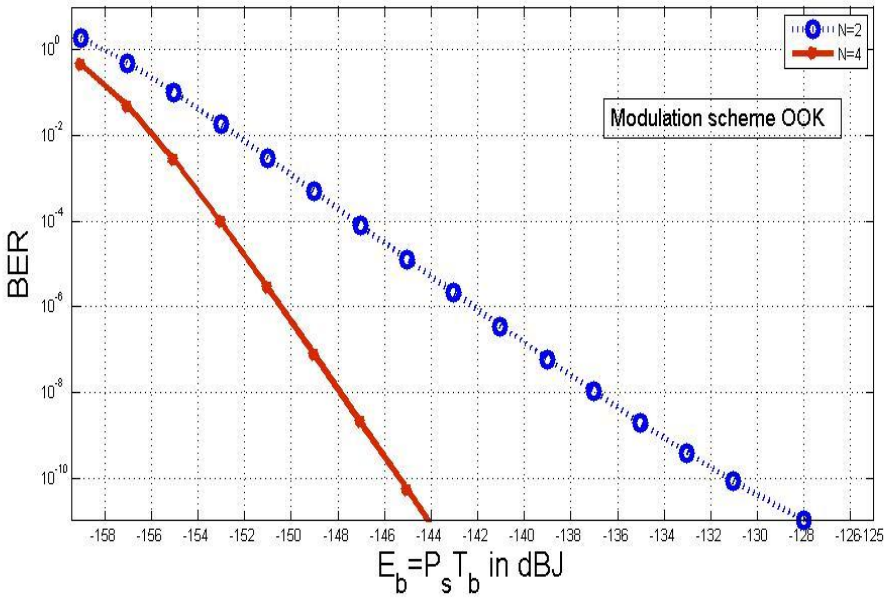

Fig. 4.14 BER versus Transmitted power for SIMO FSO link

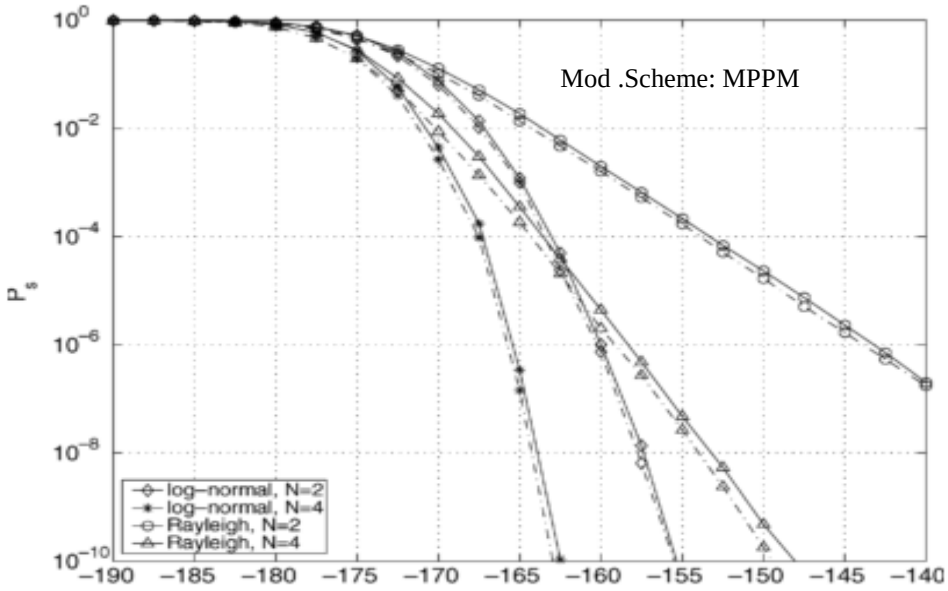

Fig. 4.15 Symbol error probability for optimal combining (dashed-dot line) and equal-gain combining (solid line), Rayleigh and log-normal (S.I. = 1) fading, and background radiation, $Q = 8$, $w = 4$, $M = 1$, and $P_bT_b = -170$ dBJ[50].

The results of BER versus energy over a bit E_b for the OOK and M-array PPM are compared in Fig. 4.14 and Fig. 4.15 following reference [50]. It is observed that there are significant improvements in receiver sensitivity due to increase in the number of receiving antenna. The trends in sensitivity improvements for OOK system are found to be similar to that for MPPM (16 dB) system although MPPM shows higher amount of improvement by almost 7.8 dB at a BER of 10^{-6}.

Chapter 5

Conclusion and future work

CHAPTER 5

CONCLUSION AND FUTURE WORK

5.1 Conclusion

A detailed analytical approach is presented to evaluate the bit error rate performance degradation of a wireless optical link in the presence atmospheric turbulence with OOK scheme and considering the STBC. The analysis is extended for different turbulence channel like log-normal and gamma-gamma channel. Evaluated performance result diversity reception in the receiver with Maximal ratio combining technique. Derived the expression of the receiver output for several sets of space time block codes with considering the Rayleigh fading Channel. The essential contributions and summary of the project are discussed below.

- It is found that performance of FSO is very sensitive to atmospheric turbulence for OOK modulation schemes. There is a significant degradation in BER performance due to heavy atmospheric turbulence and the penalty is higher for higher value of turbulence variation.

- A free space optical communication system with more than one transmitter and receiver can improve the performance as compared to the single transmitter and single receiver.

- For using MIMO technique, the signal performance is being improved in terms of BER in the presence of atmospheric turbulence.

- We have found out the unconditional bit error rate (BER) with Maximal Ratio Combining technique.

- We have determined the optimum design parameter for specific BER considering the Space time block code.

5.2 Scope for future research work

In this project, we have considered the effect of atmospheric turbulence on FSO link with spatial diversity over turbulence channel with space time block code.

Further research can be carried out to investigate the performance of WDM free space optical link considering the effect of atmospheric turbulence and pointing errors without and with Space time block code.

Further research can also be carried out on the effect of backscattering atmospheric scintillation for multi-hop FSO link with MIMO optical space time block code.

Appendix

SISO without Atmospheric Turbulence code

```
psdbm =[-28 -27 -26 -25 -24 -23 -22 -21 -20 -19];
for j=1:10
Rd=0.8;
Ps(j)=10.^(psdbm(j)/10).*(10.^-3);
Is(j)=Rd.*Ps(j);
end
e=1.6*10^-19;
k=1.38*10^-23;
T=300;
B=1*10^9;
RL=50;
varth=(4*k*T*B)/RL;
for i=1:10
I0=Ps(i);
Is(i)=Rd*I0;
Psig(i)=Is(i)^2;
Pshot(i)=2*e*Rd*I0*B;
Pth=varth;
snr(i)=Psig(i)/(Pshot(i)+Pth);
ber(i)=0.5*erfc(sqrt(snr(i)/2));
end
semilogy(psdbm,ber);
grid on
xlabel('dbm')
ylabel('BER')
title('BER versus Ps(dBm) without turbulence')
```

SISO with Atmospheric Turbulence code

```
psdbm=[-32 -30 -28 -26 -24 -22 -20 -18 -16 -14];
for j=1:10
   Rd=0.8;
Ps(j)=10.^(psdbm(j)/10).*(10.^-3);
Is(j)=Rd.*Ps(j);
end
e=1.6e-19;
k=1.38*10^-23;
T=300;
B=1*10^9;
RL=50;
sigmath=(4*k*T*B)/RL;
sigma=0.125;
for j=1:10
snr(j)=Is(j).^2/((2*e*Is(j)*B)+sigmath);
xmin=.01;
xmax=10;
N=1024;
delx=(xmax-xmin)/N;
s(1)=0.0;
for i=2:N
s(i)=0.0;
x(i)=(i-1)*delx;
I0=Ps(j);
c1(i)=(2.303*log(1+x(i))+(0.5*sigma^2))^2;
c2(i)=c1(i)/(2*sigma^2);
c3(i)=(I0+I0*x(i))*sqrt(2*pi*sigma^2);
c4(i)=exp(-c2(i));
pr(i)=c4(i)/c3(i);
pe(i)=0.5*erfc(sqrt(snr(j)*x(i))/sqrt(2));
s(i)=pe(i)*pr(i);
end
ber(j)=trapz(s);
ber(j)=ber(j)*delx;
end
semilogy(psdbm,ber);
grid on
xlabel('dbm')
ylabel('BER')
title('BER versus Ps(dBm) with turbulence')
```

SIMO with Atmospheric Turbulence code

```
psdbm =[-30 -28 -26 -24 -22 -20 -18 -16 -14 -12 -10 -8 -6 -4 -2 1 3 5  8 10 12 15 18 22
26 28 34 38 43 50 55 60 65];
for j=1:33
   Rd=0.8;
Ps(j)=10.^(psdbm(j)/10).*(10.^-3);
Is(j)=Rd.*Ps(j);
end
e=1.6*10^-19;
k=1.38*10^-23;
T=300;
B=1*10^9;
RL=50;
varth=(4*k*T*B)/RL;
sigma=.625;
for j=1:33
xmin=.01;
xmax=10.0;
N=1024;
delx=(xmax-xmin)/N;
s(1)=0.0;
for i=2:N
s(i)=0.0;
x(i)=(i-1)*delx;
I0=Ps(j);
Is(i)=Rd*I0*(1+x(i));
Psig(i)=Is(i)^2;
Pshot(i)=2*e*Rd*I0*(1+x(i))*B;
Pth=varth;
snr(i)=Psig(i)/(Pshot(i)+Pth);
L=1;
tc=snr(i)./L;
mu=sqrt(tc./(1.+tc));
a=(0.5.*(1-mu)).^L;
b=(0.5.*(1+mu));
p=0;
for q = 0:L-1
p=p+((factorial(L-1+q)/(factorial(q)*factorial(L-1))).*(b.^L));
end
pe(i)=a.*p;
%snr(i)=(Rd*I0*(1+x(i)))^2/((2*e*Rd*I0*(1+x(i))*B));
c1(i)=(2.303*log(1+x(i))+(0.5*sigma^2))^2;
c2(i)=c1(i)/(2*sigma^2);
c3(i)=(I0+I0*x(i))*sqrt(2*pi*sigma^2);
```

```
c4(i)=exp(-c2(i));
pr(i)=c4(i)/c3(i);
s(i)=pe(i)*pr(i);
end
ber(j)=trapz(s);
ber(j)=ber(j)*I0*x(i);
end
semilogy(psdbm,ber);
grid on
xlabel('dbm')
ylabel('BER')
title('BER versus Ps(dBm) with turbulence')
```

MISO with Atmospheric Turbulence code

```
psdbm =[-30 -28 -26 -24 -22 -20 -18 -16 -14 -12 -10 -8 -6 -4 -2 1 3 5  8 10 12 15 18 22
26 28 34 38 43 50 55 60 65];
for j=1:33
   Rd=0.8;
Ps(j)=10.^(psdbm(j)/10).*(10.^-3);
Is(j)=Rd.*Ps(j);
end
e=1.6*10^-19;
k=1.38*10^-23;
T=300;
B=1*10^9;
RL=50;
varth=(4*k*T*B)/RL;
sigma=.325;
for j=1:33
xmin=.01;
xmax=10.0;
N=1024;
delx=(xmax-xmin)/N;
s(1)=0.0;
for i=2:N
s(i)=0.0;
x(i)=(i-1)*delx;
I0=Ps(j);
Is(i)=Rd*I0*(1+x(i));
Psig(i)=Is(i)^2;
Pshot(i)=2*e*Rd*I0*(1+x(i))*B;
Pth=varth;
h=.9;
h1=0;
M=2;
for k=1:M
h1=h1+h;
end
snr(i)=Psig(i)*h1/(Pshot(i)+Pth);
L=1;
tc=snr(i)./L;
mu=sqrt(tc./(1.+tc));
a=(0.5.*(1-mu)).^L;
b=(0.5.*(1+mu));
p=0;
for q = 0:L-1
p=p+((factorial(L-1+q)/(factorial(q)*factorial(L-1))).*(b.^L));
end
```

```
pe(i)=a.*p;
%snr(i)=(Rd*I0*(1+x(i)))^2/((2*e*Rd*I0*(1+x(i))*B));
c1(i)=(2.303*log(1+x(i))+(0.5*sigma^2))^2;
c2(i)=c1(i)/(2*sigma^2);
c3(i)=(I0+I0*x(i))*sqrt(2*pi*sigma^2);
c4(i)=exp(-c2(i));
pr(i)=c4(i)/c3(i);
s(i)=pe(i)*pr(i);
end
ber(j)=trapz(s);
ber(j)=ber(j)*I0*x(i);
end
semilogy(psdbm,ber);
grid on
xlabel('Ps(dbm)')
ylabel('BER')
title('BER versus Ps(dBm) with turbulence')
```

MIMO with Atmospheric Turbulence code

```
psdbm =[-30 -28 -26 -24 -22 -20 -18 -16 -14 -12 -10 -8 -6 -4 -2 1 3 5  8 10 12 15 18 22
26 28 34 38 43 50 55 60 65];
for j=1:33
   Rd=0.8;
Ps(j)=10.^(psdbm(j)/10).*(10.^-3);
Is(j)=Rd.*Ps(j);
end
e=1.6*10^-19;
k=1.38*10^-23;
T=300;
B=1*10^9;
RL=50;
varth=(4*k*T*B)/RL;
sigma=.125;
for j=1:33
xmin=.01;
xmax=10.0;
N=1024;
delx=(xmax-xmin)/N;
s(1)=0.0;
for i=2:N
s(i)=0.0;
x(i)=(i-1)*delx;
I0=Ps(j);
Is(i)=Rd*I0*(1+x(i));
Psig(i)=Is(i)^2;
Pshot(i)=2*e*Rd*I0*(1+x(i))*B;
Pth=varth;
h11=.8;
h12=.7;
h13=.6;
h14=.5;
h21=.4;
h22=.9;
h23=.5;
h24=.4;
h=0;
M=2;
for k=1:M
end
N1=2;
for q=1:N1
z=(h+(h11)^2+(h12)^2+(h13)^2+(h14)^2+(h21)^2+(h22)^2+(h23)^2+(h24)^2);
z1=sqrt(z);
```

```
end
snr(i)=Psig(i)*z1/(Pshot(i)+Pth);
L=2;
tc=snr(i)./L;
mu=sqrt(tc./(1.+tc));
a=(0.5.*(1-mu)).^L;
b=(0.5.*(1+mu));
p=0;
for q = 0:L-1
p=p+((factorial(L-1+q)/(factorial(q)*factorial(L-1))).*(b.^L));
end
pe(i)=a.*p;
%snr(i)=(Rd*I0*(1+x(i)))^2/((2*e*Rd*I0*(1+x(i))*B));
c1(i)=(2.303*log(1+x(i))+(0.5*sigma^2))^2;
c2(i)=c1(i)/(2*sigma^2);
c3(i)=(I0+I0*x(i))*sqrt(2*pi*sigma^2);
c4(i)=exp(-c2(i));
pr(i)=c4(i)/c3(i);
s(i)=pe(i)*pr(i);
end
ber(j)=trapz(s);
ber(j)=ber(j)*I0*x(i);
end
semilogy(psdbm,ber);
grid on
xlabel('Ps(dbm)')
ylabel('BER')
title('BER versus Ps(dBm) with turbulence')
```

References:

[01] S. Hranilovic, Wireless optical communication system, Spring, 2005. J.E. C.G. Gunther and T. Hatori," Overview of wireless personal communicatios," IEEE commun. Mag. Vol. 33, no. 1 , PP. 28-42, 1995.

[02] D.C. Cox, " wireless personal communications: what is it?", IEEE personal commun. Mag,Vol. 2, no. 2 , PP. 20-35, 1995.

[03] R.O LaMaire, A. Krishna P. Bhagwat and J. Panian, Wireless LANs And mobile networking:Standards and future directions," IEEE personal commun. Mag. ,Vol. 2, no. 2 , PP. 20-35,1995.

[04] K. Pahlavan, A. zahedi and p. Krishnamurthy, " wideband local access wireless LAN and wireless atm," IEEE commun. Mag.,Vol. 35, no. 11 , PP. 34-40,1997.

[05] T. Standage, The Victorian Internet: the remarkable story of the telegraph and the nineteenth centurys on-line pioneers, Walker and co., New York, NY, 1998.

[06] A.G Bell Selenium and the photo phone. Nature, Pages 500-503, sept. 23, 1880

[07] F.R Gfeler and U. Bapst, " Wireless in – house data communication via diffuse infrared radiation", Proc. IEEE.vol.67, no. 11, pp.1474-1486, 1979.

[08] D. Kedar, and S. Arnon, " Urban Optical Wireless Communication Networks: The Main Challenges and Possible Solutions," IEEE Commun. Mag., Vol. 42, no. 42, no. 5, pp. 2-7, May 2004.

[09] L.C. Andrews, R. L. Phillips, and C.Y. Hopen, Laser Beam Scintillation with Application, Philadelphia, PA: SPIE Press, 2001,

[10] A. Al-Habash, L.C. Andrews and R. L. Phillips, " Mathematical model for the irradiance probability density function of a laser beam propagating through turbulent media," Optical Engineering , Vol. 40, No. 8, pp. 1554-1562, Aug. 2001.

[11] M. Uysal, J. Li, and M.Yu, " Error rate performance analysis of coded free-space optical links over gamma-gamma atmospjeric turbulence channels," IEEE Trans. Wireless Commun, Vol. 5, No. 6, pp. 1229-1233, June 2006.

[12] W.O. Popoola and Z. Ghassemlooy, " BPSK subcarrier intensity modulated free-space optical communications in atmospheric turbulence," journal of Lightwave Tech, Vol. 27, No. 8, pp. 967-973, April 2009.

[13] Nazmul and S. Majumder "Performance Analysis of a free- space optical communication system through atmospheric turbulence channels," M. Sc thesis, December 2008.

[14] S. Arnon, "Effects of atmospheric turbulence and building sway on optical wireless-communication systems." Optical Letters, Vol. 28, No. 2, pp. 129-131, Jan. 2003.

[15] S. Arnon, " Optimization of urban optical wireless communication systems," IEEE Trans. Wireless Commun., Vol. 2, No. 4, pp. 626-629, July 2003.

[16] D. Kedar, S. Arnon, " Optical wireless communication through fog in the presence of pointing errors." Applied Optics, Vol. 42, No. 24, pp. 4946-4954, Aug. 2003.

[17] A. A. Farid and S. Hranilovic, " Outage Capacity Optimization for Free-Space Optical Links with Pointing Errors." Journal of Lightwave Technology, Vol, 25, No.7, pp. 1702-1710, July 2007.

[18] T. A Tsiftsis, H.G Sandalidis, G. K. Karagiannidis, M. Uysal, " BER Performance of FSO Links over Strong Atmospheric Turbulence Channels with Pointing Errors." IEEE Communications Letters, Vol. 12, No. 1, pp.44-46, Jan. 2008.

[19] X. Zhu and J. M. Kahn, " Free-Space Optical Communication through Atmospheric Turbulence Channels." IEEE Trans Commun,Vol. 50, No.8, pp. 1293-1300, Aust . 2002.

[20] E. J. Shin and V. W. S. Chan, " Optical Communication over the turbulent atmospheric channel using spatial diversity," in proc. IEEE Conf. Global Commun. (GLOBECOM'02), Vol. 3, pp. 2055-2060; Nov. 2002.

[21] E. J. Shin and V. W. S. Chan, " part 1: Optical Communication over the clear turbulent atmospheric channel using spatial diversity," in proc. IEEE J. Select. Areas Commun, Vol. 22, No. 9, pp. 1896-1905, Nov. 2004.

[22] S. G. Wilson, M. Brandt-pearce, Q. Cao and M. Beadle, " Optical repetition MIMO transmission with multiple PPM," IEEE Trans. J. Select.Areas Commun, Vol. 9, No.23, pp. 1901-1910, Sept. 2005.

[23] S. G. Wilson, M. Brandt-pearce, Q. Cao and J.H Leveque-III, " Free-Space Optical MIMO transmission with Q-ary PPM," IEEE Trans. Commun, Vol. 53, No.08, pp. 1402-1412, Aug. 2005.

[24] S. M. Navidpour, M.Uysal and M. Kavehrad, " BER performance of Free-Space Optical transmission with spatial Diversity," IEEE Trans. Wireless Commun, Vol. 6, No.8, pp. 2813-2819, Aug. 2007.

[25] T. A. Tsiftsis, H. G. Sandalidis, G. K. Karagianidis, M. Uysal, " Optical Wireless Links with Spatial diversity over strong Atmospheric Turbulence channels." IEEE Trans.Wireless Commun.Volume 8, Number 2,pp. 951-957, Feb. 2009.

[26] E. Bayaki, R. Schober, R. K. Mallik, " Performance analysis of MIMO Free-Space optical systems in Gamma-Gamma fading ," IEEE Trans. Commun, Volume. 57, Number 11, pp. 3415-3424, Nov. 2009.

[27]. A. G. Zambrana, "Error Rate Performance for STBC in free space Optical communications through Strong Atmospheric Turbulence," vol. 11, no. 5, pp. 390-392, May 2007.

[28] Xueying Wu and peng Liu, A study on Atmospheric Turbulence Effects in full- Optical free space Communication Systems, WiCOM, pp. 1-5, Sept. 2010.

[29] S. Bloom, E. Korevaar, J. Schuster, H. Willebrand, " Understanding the performance of free-space optics ," Opt. Soc. America, Vol 2, No.06, pp. 178-200, June 2003.

[30] S. Hranilovic, wireless optical communication System , Spring,2005. J.E Padgett, C.G. Gunther and T. Hatori, " Overview of wireless personal communication," IEEE Commun. Mag., vol. 33, no. 1, pp. 28-41,1995.

[31] J. M. Kahn and J. R. Barry. " Wireless infrared communications." Proceedings of the IEEE, 85 (2): 263-298, February 1997.

[32] J. B. Carruthers and J.M. Kahn, Zhu and J. M. Kahn, "Modeling of nondirected wireless infrared channels." IEEE Transactions on Communications,Vol. 45, no.10, pp.1260-1268, October 1997.

[33] M. R. Pakravan, M. Kavehrad, and H. Hashemi." Indoor wireless infrared channel characterization by measurements." IEEE Transaction on Vehicular Technology,vol. 50, No.4, pp. 1053-1073, July 2001.

[34] G. Yun and M. Kavehrad, " Spot-diffusing and fly-eye receivers for indoors for infrared wireless communications." In Proceedings of the IEEE International Conference on Selected Topics in wireless Communications, pp. 262-265, 1992.

[35] J. B. Carruthers and J.M. Kahn, "Angle diversity for nondirected wireless communication." IEEE Transactions on Communications,Vol. 48, no.6, pp.960-969, June 2000.

[36] V. Jungnickel, A. forch, T. Haustein, U. Krger, V. Pohl and C. vou Helmolt, "Electronic tracking for wireless infrared communications." IEEE Transactions on wireless Communications,vol. 2,no.5, pp.989-999, September 2003.

[37] D. J.T. Heatley, D. R. Wisely, I.Neild, and P. Cochrane, " Optical wireless: The story so far," IEEE Communications Magazine, Pages 72-82, December 1998.

[38] Gilbert N. plass and George W. Kattawar, Influence of single scattering Albedo on Reflected and transmitted light from clouds/Applied optics 361/ vol.7 No.2/February 1968.

[39] Xiaoming Zhu and joseph M. Kahn, Fellow, IEEE, Free Space Optical Communication through Atmospheric Turbulence Channels, IEEE Transaction on communication, vol.50, no .8, August 2002.

[40] H. Manor and S. Arnon, " Performance of an optical wireless communication system as a function of wavelength ," multiscattering App. Opt. /vol. 42, no. 21, pp. 4285-4294, July 2003.

[41] Isaac I. Kim, Bruce McArthur, and Eric Korevaar, "Comparison of laser beam propagation at 785 nm 1550 nm in fog and haze for optical wireless communications," Optical Wireless Communications III, vol. 4214, pp.26-37, February 2001.

[42] D. Kedar and S. Arnon, Evalution of coherence interference in optical wireless communication through multiscattering channels,Applied optics /Vol.45, No. 14/ 10 May 2006.

[43] D. G. Breman. Linear diversity combining techniques. Proceedings of the IRE, 47:1075-1102, June 1959.

[44] S.M Alamouti " A simple Transmit Diversity Technique for wireless Communications", IEEE Journal on select area in communications,vol.16, No.8, pp.1451-1458,October 1998.

[45] Strobehn, J.W. (ed.).Topics in Applied Physics, Vol. 25, Laser Beam Propagation in the Atmosphere. Springer-Verlag: New York, 1978.

[46] Md. R. Hasan, L.H Reza and S. Majumder, "Performance Analysis on Free space MIMO Optical Wireless link over strong Atmospheric Turbulences," B.Sc Thesis, 2011

[47] X.Tang, S. Rajbhandari, W.O. Popoola, Z.Ghassemlooy, S.S Muhammad, E. Leitged and G. Kandus, "Performance of BPSK Subcarrier Intensity Modulation free-Space Optical Communications Using Log-Normal AtmosphericTurbulence Model," Photonics and Optoelectronic (SOPO), pp. 1– 4, June 2010.

[48] Sadia and S. Majumder , "Performance Analysis of a MIMO FSO system in presence of pointing error," Proceedings of 2011 International Conference on Computer Communication Management (ICCCM 2011), ISBN 978-1-84626, Sydney, February, 2010.

[49] Jon W. Mark and Weihua Zhuang, "Wireless Communications and Networking: ", Prentice Hall Inc, 2003.

[50] Stephen G. Wilson Member, Maite Brandt-Pearce, Qianling Cao and Michael Baedke, " Optical Repetition MIMO Transmission With Multipulse PPM," IEEE Journal on selected areas in communications, vol. 23, no. 9, September 2005.

.

.